

Journal Pre-proof

Assessing functionality during the early Acheulean in level TKSF at Thiongo Korongo site (Olduvai Gorge, Tanzania)

Joaquín Panera, Susana Rubio-Jara, Manuel Domínguez-Rodrigo, José Yravedra, Eduardo Méndez-Quintas, Alfredo Pérez-González, Patricia Bello-Alonso, Abel Moclán, Enrique Baquedano, Manuel Santonja

PII: S1040-6182(19)30749-9

DOI: <https://doi.org/10.1016/j.quaint.2019.09.013>

Reference: JQI 7979

To appear in: *Quaternary International*

Received Date: 6 May 2019

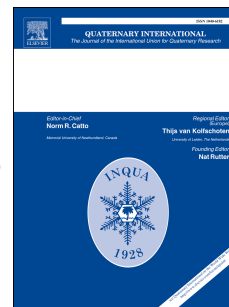
Revised Date: 9 August 2019

Accepted Date: 16 September 2019

Please cite this article as: Panera, J., Rubio-Jara, S., Domínguez-Rodrigo, M., Yravedra, J., Méndez-Quintas, E., Pérez-González, A., Bello-Alonso, P., Moclán, A., Baquedano, E., Santonja, M., Assessing functionality during the early Acheulean in level TKSF at Thiongo Korongo site (Olduvai Gorge, Tanzania), *Quaternary International*, <https://doi.org/10.1016/j.quaint.2019.09.013>.

This is a PDF file of an article that has undergone enhancements after acceptance, such as the addition of a cover page and metadata, and formatting for readability, but it is not yet the definitive version of record. This version will undergo additional copyediting, typesetting and review before it is published in its final form, but we are providing this version to give early visibility of the article. Please note that, during the production process, errors may be discovered which could affect the content, and all legal disclaimers that apply to the journal pertain.

© 2019 Published by Elsevier Ltd.



1 **Assessing functionality during the early Acheulean in level TKSF at Thiongo Korongo**
2 **site (Olduvai Gorge, Tanzania)**

3 Joaquín Panera^{1,2*}, Susana Rubio-Jara^{1,2}, Manuel Domínguez-Rodrigo^{2,3}, José Yravedra³,
4 Eduardo Méndez-Quintas⁴, Alfredo Pérez-González^{2,5}, Patricia Bello-Alonso^{1,2}, Abel Moclán^{1,2},
5 Enrique Baquedano^{2,6}, Manuel Santonja^{1,2}.

6 ¹ Centro Nacional de Investigación sobre la Evolución Humana (CENIEH). Paseo Sierra de Atapuerca, nº3,
7 09002, Burgos, Spain.

8 ² Instituto de Evolución Humana en África, Covarrubias 36, 28010, Madrid, Spain.

9 ³ Departamento de Prehistoria, Universidad Complutense, Prof. Aranguren s/n, 28040, Madrid, Spain.

10 ⁴ Grupo de Estudios de Arqueología, Antigüidade e Territorio (GEAAT), Universidad de Vigo, Facultad de
11 Historia. Campus As Lagoas, 32004, Ourense, Spain.

12 ⁵ Asociación Nacional El Hombre y El Medio, 28982, Madrid, Spain.

13 ⁶ Museo Arqueológico Regional, Plaza de las Bernardas s/n, 28801, Alcalá de Henares, Spain.

14

15 * Corresponding author. E-mail: joaquin.panera@cenieh.es

16

17 **Abstract**

18 To understand the identity of the early Acheulean, it is necessary to discriminate between the
19 variables that influenced the selection of technological strategies. Functionality of the
20 archaeological sites is crucial in assessing the manufacturing strategies of lithic tools. To
21 achieve this goal, analysis of the post-depositional processes must be evaluated. When bone
22 remains have been preserved, anthropic animal processing can be identified through
23 zooarchaeological and taphonomic analyses, and the spatial relationships among all the
24 components can also be assessed, especially when bone surface is not sufficiently preserved.

25 There are two levels present at Thiongo Korongo, ~1.3 Ma, TKLF and TKSF. These are in
26 autochthonous position with no significant temporal diachrony but with substantial
27 technological differences in the manufacturing of the lithic tools, which enables the analysis of
28 the influence of human activities on technological behaviour. In order to evaluate this issue at
29 TKSF, we present lithic, faunal, taphonomic, fabric, and spatial analyses.

30 An assemblage of megaherbivores, among which *Sivatherium* is outstanding, dominate the
31 TKSF faunal remains. Cortical preservation is poor; there is no intervention of carnivores, the
32 rate of green fractures is low, and a few cut marks on size 5 and 3b animals were identified.
33 Hence, apparently human intervention on the fauna was not intensive. Spatial and
34 geostatistical analyses hints of a specific area where megaherbivores were processed by
35 humans. Through wear use and biomarker analyses on stone tools, we are currently trying to
36 understand the activities that were carried out in the remaining paleosurface.

37 At paleosurface TKLF, the main anthropogenic input could be related to activities other than
38 animal resource exploitation, in which large handaxes were necessary. Without the
39 assessment of site functionality and chronological context, this data could have lead to the
40 differences observed at TKLF and TKSF being attributed to different Acheulean stages.

41 **Key words**

42 Early Stone Age, Spatial Analysis, Acheulean Site Function, Lithic Technology, Faunal Analysis,
43 Taphonomy.

44 **1. Introduction**

45 In the last two decades, information related to the emergence of the Acheulean has increased
46 substantially. The current geochronological framework places the onset of the Acheulean in
47 East Africa around 1.7/1.6 Ma at Kokiselei 4 at West Turkana, KGA6-A1 and KGA4-A2 at Konso,
48 FLK West at Olduvai Gorge, BSN-12 and OGS-12 at Gona and Garba IVD at Melka Kunture
49 (Quade et al., 2004; Beyene et al., 2013; Gallotti, 2013; Diez-Martín et al., 2015; Gallotti and
50 Mussi, 2018a). Apart from those, there are not many sites with this technocomplex older than
51 1.2 Ma: KGA10-A11, KGA7-A1, A2, A3, KGA12-A1 at Konso (Beyene et al., 2013), BSN-12 at
52 Gona (Quade et al., 2004), perhaps Gadeb 2 and 8 (Kurashina, 1978; Clark and Kurashina,
53 1979; de la Torre, 2011), Okote Member at Koobi Fora (Brown and McDougall, 2011),
54 Nyabusosi 18 (Texier, 1995; 2005), Type Section Complex, Lepolosi, and Noolchalai at Peninj
55 (1.5-1.4 Ma according Isaac and Curtis, 1974; Domínguez-Rodrigo et al., 2009 or 1.2/1.1 Ma
56 according Deino et al., 2006), and Bed II at Olduvai Gorge, with the largest cluster composed of
57 EF-HR, SHK, BK, FC West OF, and TK (Leakey, 1971; de la Torre et al., 2018; Santonja et al.,
58 2014; Domínguez-Rodrigo et al., 2013; Diez-Martín et al., 2014). In the Eastern African
59 sequences, there is a gap in the Acheulean archaeological record between ~1.2 and 1 Ma
60 (Hay, 1994; Roche et al., 2003; Quade et al., 2008; Beyene et al., 2013; Clark and Kurashina,
61 1979), which allows us to distinguish chronologically the groups of Acheulean sites dated
62 between 1.7 and 1.2 Ma from the later ones.

63 Knowledge of the Acheulean Technocomplex comes mainly from the technological analysis of
64 the lithic industry (Gallotti, 2013; Diez-Martín et al., 2015; Beyene et al., 2013; Quade et al.,
65 2004; de la Torre, 2011; Texier, 1995; Diez-Martín et al., 2018; Leakey, 1971; de la Torre et
66 al., 2018; Santonja et al., 2014; 2018; Domínguez-Rodrigo et al., 2013; Diez-Martín et al., 2014;
67 Rubio-Jara et al., 2017). Differences in the manufacturing strategies of lithic tools have been
68 established between the Acheulean sites older than 1.2 Ma and the younger ones (de la
69 Torre and Mora, 2005; Sharon, 2007; 2010; Stout, 2011; Diez-Martín and Eren, 2012; Beyene
70 et al., 2013; Sahnouni et al., 2013; Gallotti, 2013; Gallotti and Mussi, 2017, 2018a; Texier,
71 2018), perhaps not taking into consideration other variables that may influence those
72 strategies, such as cultural traditions, quality and availability of raw material, functionality, etc.

73 Among these variables, functionality of the archaeological sites is determinant (Presnyakova et
74 al., 2018), although this has been very rarely tackled, partly because most of these sites are
75 more or less affected by hydraulic transport (Domínguez-Rodrigo et al., 2009; Gibbon et al.,
76 2009; Diez-Martín and Eren, 2012; Gallotti, 2013; Diez-Martín et al., 2014; Uribe Larrea et al.,
77 2017; de la Torre et al., 2018; Semaw et al., 2018).

78 Functional analysis must be based on the analysis of the post-depositional processes that form
79 the archaeological assemblages (Diez-Martín and Eren, 2012), particularly in the early
80 Acheulean sites, as many of them are found in alluvial environments, in which taphonomic
81 processes have rarely been taken into consideration (Petraglia and Potts, 1994). In those cases
82 where bone remains are present, the zooarchaeological and taphonomic analyses enable the
83 identification of anthropic activities related to animal processing, however preservation of the
84 bones is not always ideal for an adequate analysis of bone surface modifications. Thus, in order
85 to establish relationships between lithic industry and fauna, or among other elements, after

86 the analysis of completeness of the archaeological level, the spatial relationships among all the
87 components must be assessed. The associations in the graphic display of spatial analyses are
88 more complex and subtle than what can be visually inferred. Spatial statistical tests have been
89 developed within the fields of earth sciences, health, and economy, and have become
90 essential for the study of spatial distribution in archaeology (Baddeley et al., 2015; Bivand,
91 2010; Dorman, 2014; Pebesma, 2004; Roger et al., 2013). The analysis of spatial distribution
92 has a great potential to reach conclusions regarding social behaviour, based on the bones and
93 lithic tools abandoned by the hominins. Thus, research on ethnoarchaeological, social
94 behaviour and spatial distribution experienced a great surge in the late 70's and 80's of the
95 20th century (Binford, 1978; Hodder and Orton, 1976, Yellen, 1977). Over 25 years after the
96 first works with statistical application to spatial analysis (Whallon, 1973, Whallon, 1974), there
97 are more powerful statistical tools used in spatial analyses that can be applied to archaeology
98 (Bivand, 2010; Dray et al., 2012; Pebesma, 2004; Roger et al., 2013). These analyses allows the
99 objective determination of the presence and degree of spatial interdependences among the
100 different elements of the archaeological record (Domínguez-Rodríguez and Cobo, 2017).

101

102 As has been pointed out, the highest concentration of early Acheulean sites has been recorded
103 in Bed II at Olduvai Gorge (Leakey, 1971; Santonja et al., 2014; Diez-Martín et al., 2009, 2014,
104 2015; Sánchez-Yustos et al., 2016; Rubio-Jara et al., 2017; de la Torre et al., 2018), and the
105 time span between 1.69 Ma y 1.34 Ma encompasses the whole chronological frame of the
106 early Acheulean. Such characteristics allow the analysis of the variability of this technocomplex
107 during its early stages in a confined geographical frame, with similar availability of lithic raw
108 materials.

109 At Thiongo Korongo (TK), ~1.3 Ma, one of the highest concentrations of Acheulean lithic tools
110 of the early Acheulean has been preserved (Leakey, 1971; Santonja et al., 2014) in
111 autochthonous position, together with a large number of bones (Yravedra et al., 2016). The
112 remains are allocated mainly on two stratigraphically close paleosurfaces, named TK Lower
113 Floor (TKLF) and TK *Sivatherium* Floor (TKSF). Substantial technological differences can be
114 distinguished in the manufacturing of the lithic tools (Rubio-Jara et al., 2017), which enables
115 the analysis of the influence of the human occupations' functionality on the technological
116 strategies implemented in the manufacturing of lithic tools during the early Acheulean.

117 In order to evaluate the effects of the functionality of the sites on the technological strategies
118 for the first time, this paper presents the zooarchaeological and taphonomic study of the bone
119 remains and stone tools recorded in the 45.3 m² excavated of the TKSF, the geoarchaeological
120 analysis of this level; its depositional patterns and degree of disturbance, the analysis of the
121 spatial integrity, the spatial distribution of faunal and lithic remains, as well as the statistical
122 spatial analysis with the aim of objectively determining whether or not spatial
123 interdependences of different types of archaeological remains exist, and how this dependence
124 is expressed by clusters or regularity (Domínguez-Rodrigo and Cobo-Sánchez, 2017).

125 2. Thiongo Korongo Site and TKSF level

126 TK is located 2 km east of the junction of the Main and Side Gorges at Olduvai,
127 Tanzania (Fig. 1a). From a stratigraphic point of view, it is located in Upper Bed II, nearby and
128 adjacent to Bed III. It can be related to Tuff IID, and dated by ⁴⁰Ar/³⁹Ar to 1.353±0.035 Ma
129 (Domínguez-Rodrigo et al., 2013).

130 The site was identified in 1931 by L. Leakey (Leakey, 1951), although not excavated
131 until 1963 (Leakey, 1971), when M. Leakey dug two areas: Trench I, of 46.4 m², and Trench II,
132 of 40.5 m², four meters apart. An approximately five-meter-thick stratigraphic sequence
133 consisting of levels of tuff, clays, and calcareous crusts was described (Hay, 1976). Two main
134 archaeological levels were identified: TK Lower Floor (TKLF) and TK Upper Floor (TKUF), which
135 were considered true clay surfaces characterized by large industrial assemblages and a smaller
136 amount of faunal remains. TKLF was interpreted as Acheulean, and TKUF as Developed
137 Oldowan B (Leakey, 1975: 484, 1976: 31, 1978). From then on, TK played a decisive role in the
138 debate about the relationship between the Oldowan and Acheulean (Bower, 1977; Stiles,
139 1977, 1979; Willoughby, 1987; Sahnouni, 1991; Ludwig and Harris, 1998; Kimura, 2002). Later
140 research came to the conclusion that both industrial assemblages were technologically similar
141 and could be ascribed to the Acheulean technocomplex (de la Torre, 2004; de la Torre and
142 Mora, 2005).

143 In 2010, in the framework of The Olduvai Paleoanthropology and Paleoecology Project
144 (TOPPP), a new research phase that is still ongoing commenced. The stratigraphic section
145 established by our field work, combined with the sections referred to by M. Leakey (1971: 172-
146 174), has allowed the reinterpretation of the stratigraphy of the site (Santonja et al., 2014), to
147 verify that it is more complex than was previously thought (Rubio-Jara et al., 2017), and to
148 correct mistakes made in previous interpretations, particularly related to TKUF which was
149 mixed up with TKLF (Santonja et al., 2014; 2018). A new archaeological floor placed between
150 TKLF and TKUF, named TK *Sivatherium* Floor (TKSF), unrecorded in M. Leakey and R. Hay's
151 stratigraphic sequence (Leakey 1971: 172 ff), has been identified and 45.3 m² have been
152 excavated.

153 The technological and techno-economic study of the *chaîne opératoire* phases
154 identified in TKSF (Rubio-Jara et al., 2017) reveal that this new archaeological unit shows
155 strong differences with the lithic industry and faunal remains of TKLF (Santonja et al., 2014;
156 2018; Yravedra et al., 2016). Both levels are clearly Acheulean, and are located stratigraphically
157 very close to each other (between 21 and 42 cm), with no significant temporal diachrony
158 (Rubio-Jara et al., 2017). This suggests that their technical and typological differences in the
159 context of the variability of the Acheulean assemblages are mainly due to functionality criteria.

160 **2.1. Geological context**

161 Beds II, III, and IV of the Olduvai sequences, according to the stratigraphic nomenclature of
162 Hay (1976), are displayed in the TK sedimentary outcrops. The maximum thickness recorded is
163 about 8.90 m, of which 7.25 m are Bed II, 1.25 m Bed III, and 0.40 m Bed IV. Our fieldwork in
164 the northwest part of TK carried out between 2014 and 2015 is represented to the
165 stratigraphic section of **Fig. 1b** (Rubio-Jara et al., 2017), and must be added to the previous
166 stratigraphic column (Santonja et al., 2014) and the sections documented by M. Leakey (1971:
167 172-174).

168 The TKSF occupation floor is located some 20-30 cm over the TKLF occupation floor. TKSF is
169 exposed over a paleosurface composed of two sedimentary facies associated with a 40 cm
170 thick loamy sand channel with tabular cross-stratification, internal structures, and NW-SE flow
171 (**Fig. 1b**). Judging by the narrow and shallow nature of this channel, it was seasonal and short-
172 lived, and had a low transport capacity. The base of these channel facies lie, depending on the

173 sector, over a pale yellow sandy loam tuff or a thin carbonate level. Both facies represent a
 174 very shallow lake environment. A 14 cm thick deposit of pale brown clay can be distinguished
 175 to the top of the channel facies and in the south side of the excavated area. This is interpreted
 176 as a decantation facies related to the loamy sand overbank placed in a stratigraphically lower
 177 position. On the other hand the TKSf occupation floor is covered by a horizon of white pale
 178 yellow sandy clay tuff about 25-52 cm thick, with very low erosive capacity. The uppermost
 179 part of the stratigraphic section consists of a pale yellow clay loam tuff 2-32 cm thick,
 180 truncated at the top by a cut and a fill and eroded by a new light grey clay tuff horizon which
 181 shows a marked erosive scar over the lower tuff. Several recent rills, fossilized colluvium, and
 182 soils end the section.

183 **2.2. General Characteristics of the Lithic Industry present in the TKSf**

184 A total of 1,161 lithic items were recovered from the 45.3 m² excavated at TKSf (**Fig. 2a and**
 185 **2b**). This amounts to a density of 12.1 pieces per m² excluding shatter, and 5.3 kg m² of weight
 186 including it (Rubio-Jara et al., 2017). The different items have been distinguished according to
 187 the type of raw material employed (**Table 1**), and it was found that 91% are made of quartzite,
 188 which came from the Naibor Soit Ndogo inselberg. At the time the site was formed, the base of
 189 the hill would have been about 750 m away (Santonja et al., 2014). Naibor quartzite (NQ) is a
 190 metamorphic rock composed almost entirely of quartz (98%) and has a schistose texture,
 191 which provides it with a very different knapping response compared to other fine-grained
 192 quartzites present at Olduvai (Jones, 1994). A total of eight percent of the items are “volcanic
 193 rocks” (VR) –phonolites, nephelinite, trachyte, and basalt- which come from the formations of
 194 the Olmoti, Ngorongoro, Sadiman, and Lemagrut volcanoes (Hay, 1976; Jones, 1994; Kyara,
 195 1999: 14). These volcanic rocks could have been obtained from nearby streambeds. The
 196 remaining one percent of the items are made on vesicular lava, non-Naibor quartzite (nNQ),
 197 metamorphic rocks, and gneiss. The known gneiss outcrops are located 11 km west of TK, at
 198 Kelogi Hill (Hay, 1976; Kyara, 1999).

199 NQ and VR are the only raw materials in which all the phases of the *chaînes opératoires* are
 200 represented, and the handaxes are shaped. Knapping activities at the TKSf site are focused on
 201 producing flakes from cores, occasionally reshaping them by retouch, as well as the shaping of
 202 handaxes from slabs, cobbles, and even large flakes. Direct freehand percussion (FHP)
 203 exploitation schemes have been identified on blanks obtained from these two rock types.
 204 Bipolar percussion (BP) was observed almost exclusively on NQ.

205 Over half of all the VR items are cobbles (55.4%) and were used as hammerstones. This shows
 206 the importance of percussion activities and the versatility of these blanks, which were also
 207 exploited as cores.

208 All the identified exploitation systems are recorded in both NQ and VR in TKSf. Almost two
 209 thirds of the cores were exploited according to unsophisticated operative schemes: single
 210 surfaces with monopolar or bipolar removals, multipolar and bifacial cores. However, the
 211 existence of a peripheral unipolar system in 16.3% of the cores is noteworthy (similar to the
 212 Quina production concept documented in Europe, Turq, 2000: 316). This was also recorded at
 213 TKLF (Santonja et al., 2014). Discoid productions schemes, which are the most complex ones,
 214 are highly represented (22.4%).

215 The FHP exploitation method clearly prevailed over BP (60.4% and 39.6% respectively). The
216 transfer of percussion methods has been documented, so in the 41.7% of the cores exploited
217 by BP display FHP, and in 9.1% of the ones exploited by FHP display BP. This flexibility between
218 techniques has also been confirmed among different categories of the *chaîne opératoire*, thus
219 half of the polyhedral cores show marks on several ridges that suggest that they were used as
220 hammerstones, and cores made on slabs by FHP were also used as anvils.

221 A total of 341 flakes were identified, most made of NQ (94.1%) and the rest (5.9%) made from
222 VR blanks. Ten percent of the NQ flakes and none of the VR examples are more than 100 mm
223 long, some of NQ reaching up to 160 mm. The size of the largest NQ flakes fall within the range
224 of the Large Cutting Tool (LCT) category. On the other hand, 6.5% of all flakes show debitage
225 and cortical backs, and most show a long active cutting edge, as well as use retouch and
226 extensive removals. Obtaining long active cutting edges must therefore have been a primary
227 goal in their preparation. The presence in TKSF of two VR flakes with extensive cortex, together
228 with 2.2 flakes per core and only five undifferentiated products, suggests that exploitation of
229 VR cores began outside the site or in a different sector of TKSF. However, the proportions of
230 those three categories are more consistent on NQ; 5.1 flakes per core and about 9.6
231 undifferentiated products per core suggest that blanks of NQ would have been carried out and
232 knapped on site. Consequently, at TKSF we identify an economy of production that differs for
233 VR and NQ (Rubio-Jara et al., 2017).

234 Production of retouched tools was not the main objective at the TKSF, as only nine retouched
235 items were documented: four scrapers, two denticulates, one notched tool, and two backed
236 knives.

237 The *façonnage* phase consists of 53 items that represent 9.6% of the lithic assemblage
238 (excluding undifferentiated products). Most of them (37 pieces) are handaxes. Eight trihedral
239 picks, four cleavers, and four large shaped flakes and slabs have also been recorded, despite
240 the difficulty of detaching large flakes on NQ. Whole pieces, tips and preforms (specimens in
241 an intermediate phase of shaping) have been identified among the handaxes. Three of the NQ
242 handaxes and three of the VR handaxes were made on flakes. The bilateral shaping of the NQ
243 specimens is generally bifacial, and tends to be invasive. The cutting edge that covers the tool
244 dominates the whole perimeter up to the tip, shaping the potentially sharp and active edges all
245 around the tool. The reduction method used on the silhouettes produce pointed, oval, and
246 transverse-edge handaxes. The presence of NQ handaxe preforms and points suggests that
247 such tools were shaped and used on this level, and that they could have been used for a long
248 time, as they were rejuvenated by lateral and distal sharpening removals (Rubio-Jara et al.,
249 2017; Fig 5 and 7). The trihedral picks, which are slightly smaller than the NQ handaxes, are
250 made on NQ slabs, and in half of them unifacial reduction is dominant. All cleavers are made
251 on NQ flakes (types 0, I, and II of Tixier, 1956), except for an atypical one made on a NQ slab.
252 Finally, the large scrapers and shaped slabs are usually over 10 cm long, and tend to be shaped
253 to a tip, or create cutting edges on opposite backs that form a techno-functional unit suitable
254 for gripping.

255 There is a large number (611 items) of undifferentiated products or shatter (debris, chunks,
256 and angular fragments of NQ slabs). They constitute more than half (52.6%) of the TKSF

257 assemblage, of which 99% are on NQ and only 1% on VR (Rubio-Jara et al., 2017). The high
258 occurrence of shatter may be produced mainly during all the phases of knapping on NQ slabs,
259 although the possibility of it resulting from percussion activities that involved NQ anvils or
260 hammerstones cannot be ruled out (Diez-Martín et al., 2011; Sánchez-Yustos et al., 2012; de la
261 Torre and Mora, 2013).

262 **3. Method and sample**

263 **3.1. Data acquisition and management**

264 The topography of TKSF, the stratigraphic data, and the archaeological materials were
265 recorded by a Leica Total Station TS02. All the information was managed using Microsoft
266 Access and Microsoft Excel, and was processed with ArcGis®. The coordinates of faunal and
267 lithic items were registered with a variable number of points according to their size and shape:
268 small items with an undefined axis were recorded as a single point; small items with a
269 silhouette suggestive of orientation were recorded with two points on the long axis; the rest of
270 the items were identified with a number of points ranging from 3 to 43. The maps were drawn
271 with ArcGis® software from the topographic data and the resulting polygon - in shape files .shp
272 – was highly accurate. The orientation and slope of the items could be recorded more
273 accurately and quickly by this method than by freehand drawing on graph paper.

274 **3.2. Faunal analysis**

275 Taxonomic identifications were carried out using comparative material, backed up with
276 osteological atlases and references (Barone, 1976; Gentry and Gentry, 1978, 1978a; Pales and
277 Lambert, 1971). However, in cases where such determination was not possible, fragments
278 were attributed to animal weight/size classes following Bunn (1982), where “small” refers to
279 Bunn’s (1982) sizes 1 (animals <50kg, such as Thompson's gazelles) and 2 (50 - 250kg, such as
280 warthogs), “medium” to size 3a (250 - 500kg, such as gnus) and 3b (500 - 700kg, such as
281 zebras), and “large” to sizes 4 (750 - 2000kg, such as elands or buffaloes), 5 (2000 - 6000kg,
282 such as rhinoceros), and 6 (>6000kg, such as elephants).

283 Faunal remains were quantified by NISP and MNI. NISP determination follows the protocol
284 described in Yravedra and Domínguez-Rodrigo (2009). MNI estimates considered element size
285 and ontogenetic age (Brain, 1969). Skeletal part profiles were organized into four different
286 anatomical regions: cranial (i.e., horn, cranium, mandible, and teeth), axial (vertebrae, ribs,
287 pelvis, and scapula, according to Yravedra and Domínguez-Rodrigo, 2009), upper appendicular
288 limbs (humerus, radius, ulna, femur, patella, and tibia), and lower appendicular limbs
289 (metapodial, carpals, tarsals, phalanges and sesamoids).

290 Pursuant to Yravedra et al (2016), several procedures were followed to reconstruct site
291 formation processes, assess site integrity, and evaluate the contribution of various biogenic
292 agents to the faunal assemblage. The impact of water activity was estimated based on
293 fragment size distributions and the presence of abrasion, polishing, and carbonates.

294 The analysis of animal sizes was carried out at three levels. First, all fragments were subjected
295 to size-sorting. With regard to bone fragmentation indices, bones were separated into several
296 categories according to their maximum length: <20mm, 21-40mm, 41-60mm, 61-80mm, 81-
297 100mm, and >101mm. At a second level, only long bone fragments were considered, as

298 cancellous axial bones undergo different fragmentation patterns than do denser limb bones
299 (Domínguez-Rodrigo and Martínez-Navarro, 2012). Based on the idea that anthropogenic bone
300 concentrations yield greater fragmentation than those created by carnivore, the amount of
301 preserved shaft circumference is also considered. Bunn (1982) proposed three categories for
302 shaft circumference where (1) stands for shaft circumference <50%; (2) covers the >50% range;
303 and (3) the shaft circumference is complete (100%). At a third level, according to Villa and
304 Mahieu's (1991) classification, dry and green breakage was analysed and only those long bone
305 fragments showing green breakage were considered. This distinction is important, as
306 diagenetic (dry) breakage is relatively common in the assemblage, and thus the specimen size
307 distribution could be quite different from the original deposit.

308 Weathering stages were also observed following Behrensmeier (1978) to estimate exposure
309 time. A spatial analysis of bones with evidence of abrasion-polish, carbonate encrustation,
310 trampling-microabrasion, and biochemical marks was carried out to evaluate whether
311 taphonomic phenomena were focused on specific areas. Bone surface modifications such as
312 cut, percussion and tooth marks were systematically examined with 10X-20X hand lenses and
313 indirect lighting (Blumenshine, 1988, 1995). The diagnostic criteria defined by Bunn (1982)
314 and Domínguez-Rodrigo et al. (2009) guided the identification of cut marks, which have been
315 clearly identified as straight continuous grooves, with V section and microstriation, as
316 opposed to trampling marks, which are shallow, discontinuous grooves with open sections,
317 often associated with microabrasiones. . Tooth marks were analysed following Blumenshine
318 (1988, 1995). Finally, the identification of percussion marks was based on Blumenshine and
319 Selvaggio (1988), Capaldo and Blumenshine (1994), and Blumenshine (1995). Those tend to
320 be irregular circular marks with irregularities inside, different to carnivorous pits, which usually
321 show a flat bottom.

322 **3.3. Lithic taphonomy**

323 The analysis of the surfaces of the lithic tools allows the identification of a number of post-
324 depositional alterations, particularly when the whole lithic assemblage is affected (Harding et
325 al., 1987; Petraglia and Potts, 1994; Dibble et al., 1997; Hosfield and Chambers, 2003; Hosfield,
326 2011). Thus, breakage patterns, rounding, patina development, heat alterations, and trampling
327 analyses have been carried out (Shea, 1999; Hiscock, 2002; Burroni et al., 2002; Villa and
328 Courtin, 1983; Glauber and Thorson, 2012). Due to the particular characteristics of TKSF
329 tools, roundness and breaking patterns have been analysed at TKSF.

330 The most common alterations among the lithic industry are rounding, abrasion, chipping, and
331 pseudo-retouch (Petraglia and Potts, 1994; Shea, 1999; Bustos-Pérez et al., 2019). The
332 establishment of the degree of rounding is usually done macroscopically (Petraglia and Potts,
333 1994, Panera and Rubio-Jara, 1996; Shea, 1999), although some protocols have been
334 implemented in order to identify it microscopically (Shackley, 1974; Bustos-Pérez et al., 2019).
335 Following an initial visual inspection of the TKSF lithic industry, and having observed a low
336 rounding index in the sample, microscopic analysis was deemed necessary. Basic roundness
337 categories were established: null, light, intense, and indeterminate (Panera and Rubio-Jara,
338 1996). Chipping and pseudo-retouch have been identified and described according to intensity.

339 Broken artefacts also provide information regarding the taphonomic history of the lithic
340 assemblage. A high number of fractured pieces may suggest intense post-depositional
341 processes (Andrefsky, 2005). A lithic piece can get fractured during production or use, or due
342 to post-depositional processes (Hiscock, 2002). The mechanical particularities of NQ (Jones,
343 1994; Santonja et al., 2014; Bello-Alonso et al., submitted) often contribute to breaking during
344 the knapping process, particularly during the final stages of handaxe production (Herzlinger et
345 al., 2015). On the other hand, consumption of lithic tools has been verified in TKSF, and under
346 that activity fractures occasionally occurred (e.g. handaxe broken tips; Rubio-Jara et al., 2017).
347 Fracture analysis has been limited to flakes, taking into consideration the probabilities of
348 fracture during the knapping process.

349 **3.4. Spatial and geostatistical analyses**

350 3.4.1. Orientation and fabric analyses

351 Orientation and fabric analysis are suitable methods to assess the sedimentary and natural
352 post-depositional disturbance of archaeological assemblages (Schick, 1986; Bertran and Texier,
353 1995; Lenoble and Bertran, 2004; Domínguez-Rodrigo et al., 2012; Cobo-Sánchez et al., 2014;
354 Domínguez-Rodrigo et al., 2014; García-Moreno et al., 2016).

355 The data used to test orientation and fabric (trend and dip) were obtained with a specific
356 software GIS process. The trend was calculated with two different processes: minimum
357 bounding rectangle of a polygon (MBR) and polygon main angle (PMA), methods which have
358 already been used in similar archaeological contexts (Domínguez-Rodrigo et al., 2012;; Cobo-
359 Sánchez et al., 2014; Domínguez-Rodrigo et al., 2014).

360 The items taken into account for this analysis are those >50 mm with an elongation index (i.e.
361 = length/width) >1.6. The orientation data was evaluated with the Rayleigh and Kuiper tests to
362 differentiate uniform (isotropic) from non-uniform (anisotropic) distributions (Fisher, 1993;
363 Lenoble and Bertran, 2004).

364 In fabric analysis, the criteria are the same as in orientation analysis and we calculated some
365 fabric indexes (eigenvectors, eigenvalues, K and C ratios, Vollmer's fabric indexes) and
366 produced various graphs (stereographic projections, Woodcock and Vollmer diagrams) (Fisher,
367 1993; Lenoble and Bertran, 2004; McPherron, 2005).

368 3.4.2. Density and distribution pattern analyses

369 Density and distribution pattern analyses were calculated with ArcMap® geo-statistic tools.
370 The assemblage density was calculated through the kernel density method (Silverman, 2018),
371 the clustering degree through Nearest Neighbour and Getis General Ord G statistical methods
372 (Boots and Getis, 1988; Getis and Ord, 1992), and their spatial interrelations using K means, as
373 well as HotSpot methods (Getis and Ord, 1992). All methods are commonly used in spatial
374 analyses of Palaeolithic sites with contrasted and robust results (Romagnoli and Vaquero,
375 2016; Giusti et al., 2018).

376 3.4.3. Spatial point patterns

377 The point pattern from the archaeological level was examined to ascertain whether it was a
378 complete spatial random (CSR) process. Homogeneous CSR (i.e., homogeneous Poisson) point
379 patterns are characterized by being homogeneous (points lack spatial preference and they
380 occur proportionally in any given area according to their dimensions) and by points being

381 spatially independent. A homogeneous Poisson distribution is a uniform distribution. An
382 inhomogeneous Poisson distribution is a spatially-dependent intensity pattern. An
383 inhomogeneous Poisson pattern can be CSR if point patterns show a Poisson probability
384 distribution and if points are independent. A point pattern is stationary if point statistical
385 properties do not depend on location. This pattern is also defined as isotropic if the statistical
386 properties do not depend on the shifting or rotation of the window. CSR Poisson processes are
387 both stationary and isotropic. Inhomogeneity may create spatially-varying intensity patterns,
388 which should not be mistaken with clustering. In the former, points preserve their
389 independence. In the latter, there is spatial dependence among points.

390 It is very common to use Ripley's K-function, but this method is very sensitive to the spatial
391 variation of intensity, leading to false clustering interpretations. For this reason, we carried out
392 tests to assess whether the TK spatial pattern was a CSR Poisson process. For this purpose, we
393 used quadrat counting (chi-squared) test of homogeneity by dividing the spatial window in
394 square meter subunits. The quadrat test was used via Monte Carlo simulations ($n=500$). The
395 result was obtained by averaging all simulations. Due to limitations of the quadrat test
396 (Baddeley et al., 2015), we complemented it with a Diggle-Cressie-Loosmore-Ford (DCLF) test.
397 The DCLF test was carried out also with Monte Carlo simulations ($n=99$) and averaged results.
398 An extension of this test was also used, based on the simulation ($n=19$) of random
399 inhomogeneous Poisson processes with intensity derived by using the leave-one-out kernel
400 smoother method. We combined the use of the DCLF test with the inhomogeneous version of
401 the L-function (see below), using a global envelope. The archaeological spatial pattern was
402 compared to the resulting model.

403 A non-parametric method of kernel maps was also used to produce graphic smoothing
404 estimations of intensity. Kernel band width selection was made using automatic algorithms
405 that minimize error measurements. Diggle's correction is commonly used to minimize the edge
406 effect, but it assumes a Cox clustering process (Baddeley et al., 2015), which in the present
407 case is inadequate. For this reason, we selected a likelihood cross-validation algorithm that
408 assumes an inhomogeneous process as shown by homogeneity tests. Sometimes, fixed
409 smoothing band widths fail to capture abrupt changes in local intensity. For this reason,
410 adaptive estimators of intensity based on Dirichlet-Voronoi estimation of density are better
411 able to capture the subtleties of local variation since the resulting bandwidths are local instead
412 of the same for the whole window. The algorithm also enables averaging multiple
413 computations across the window. The adaptive density kernels allowed more precise spatial
414 delineation of regions within the area that were more intensely inhomogeneous. Here, a
415 tessellation of the intensity estimate based on a 10% fraction of the data points was used.
416 Monte Carlo simulations ($n=30$) were used to derive the final pattern.

417 The K-function measures the cumulative average number of points falling within a certain
418 radius of any given data point. This estimation is corrected for window-edge effects and
419 modified according to intensity. However, given that the K-function assumes a homogeneous
420 point process, more robust modified versions of this test exist. One of them is the L function,
421 which can adapt a centred version of the K-function, and which applies a square root
422 transformation of the Poisson K-function. This stabilizes the variance. Here, we used an
423 inhomogeneous version of the L-function. Confidence intervals apply to these functions.
424 Acceptance intervals for a CSR hypothesis using 5% significance levels were also used in our

425 analyses, by using confidence envelopes resulting from Monte Carlo bootstrap simulations.
426 Corrections for edge effect, border effect, isotropy, and translation were applied. Global
427 envelopes were selected because they include the most extreme deviations from the
428 theoretical functions.

429 Clustering was approached through Clark-Evans tests using Monte Carlo simulations ($n=300$).
430 This test produces R values from 0 (confirmation of the null hypothesis of CSR) to 1 (maximum
431 cluster). However, this test assumes homogeneity and can be biased in inhomogeneous point
432 processes. As a complement, the Hopkins-Skellam test was also used, because it is less
433 sensitive than the Clark-Evans test to inhomogeneity (Baddeley et al., 2015). This test produces
434 a value of A which indicates a random pattern ($A=1$), clustering ($A<1$), and regularity ($A>1$).

435 The TK archaeological sample was also analyzed as a multitype pattern to detect spatial co-
436 dependence between lithic and bone remains. For this purpose, an inhomogeneous cross-type
437 L -function was used. The L_{ij} indicates the association between both types of materials. If the
438 data line is outside the confidence envelope, then both types of materials are spatially
439 dependent. This can be expressed as being clustered (the probability of i points being within
440 the distance of any specific radius of j points is higher than the benchmark value) or regularly
441 spaced (the probability of i points being within the distance of any specific radius of j points is
442 lower than the benchmark value). This type of analysis is displayed in a bivariable quadruple
443 graph. The diagonal graphs (upper left and lower right) indicate the inhomogeneous L_{ii}
444 distribution. The off-diagonal graphs (upper right and lower left) indicate the inhomogeneous
445 L_{ij} association type. Global 95% confidence envelopes were used.

446 As a support to this approach, random labelling was also used via the J function. As explained
447 in (Domínguez-Rodrigo et al., 2017), $F_i(r)$ is the empty-space function for type i points. $G_{ij}(r)$ is
448 the nearest neighbour function measuring distances from points i to j . If points of type i and j
449 are independent, then $G_{ij}(r)=F_j(r)$. The J_{ij} function is the result of $1-G_{ij}(r)/1-F_j(r)$. Random
450 labelling is a stochastic method randomly allocating labels to points. This is carried out via
451 permutation tests involving Monte Carlo methods, which randomly label the original points
452 (Baddeley et al., 2015). For envelope-based tests, “dot” functions are the most adequate.
453 These functions evaluate distances from points i to any type of point. It is used to assess the
454 dependence of one type of point to the rest of the point process. This procedure is most
455 efficient in stationary processes and its selection here as a supplement to the inhomogeneous
456 K function is just to balance the different selection of variance by stationary and non-
457 stationary methods. Confidence envelopes were selected via resampling ($n=50$) Monte Carlo
458 methods.

459

460 **4. Results**

461 **4.1. Faunal analysis**

462 The taxonomic study reveals TKSF preserved a macrovertebrate accumulation, among which
463 megaherbivores are common, as several bones of *Sivatherium*, elephant, and buffalo are
464 represented (**Fig. 2c**). Other animals of medium size are also represented, such as zebra,
465 wildebeest, and *Metridiochoerus* (**Table 2**). Species of smaller sizes that could not be

466 taxonomically identified have been assembled in different categories according to their size
467 (**Table 2**).

468 Among those of medium size, size 3b animals stand out. Despite relatively low NISP values,
469 virtually all anatomical sections are represented (**Table 3**). Axial elements stand out amongst
470 the larger animals –sizes 4 and 5- due to the high number of ribs and vertebrae (**Table 3-4**).
471 Representation of axial and appendicular elements of *Sivatherium*, and dental fragments
472 together with lower appendicular elements (i.e., metapodials) of hippopotamus, are also well-
473 represented after detailed analysis of these two animals, which are the best represented
474 (**Table 4**). Nevertheless, axial bones are dominant amongst indeterminate bones of animals
475 ascribed to sizes 4 and 5.

476 In relation to bone alteration patterns, it has been stated that 70.87% of the remains show
477 poor preservation of the cortical surfaces, which has hindered observation of some bone
478 alterations. Only 16.83% of the sample is well preserved and 12.30% is moderately well-
479 preserved. Despite this data, polishing and abrasion has been identified in 81.35% of the
480 sample, which together with the high percentage of remains with concretions (72.03%)
481 suggests that the bones were exposed to hydric alterations for a prolonged time period
482 However, the nature of these alterations are shown as polishing and abrasion rather than
483 rolling, as less than 5% of bones show evidence of intense rolling (**Table 6**). The high presence
484 of polished and abraded bones, together with the scarcity of rounded bones suggest the
485 existence of water flows on site, although these were low energy. The small particles
486 transported by the streams probably gave place to abrasion and polishing, and although they
487 were not strong enough as to move the bones of macromammals, they could have displaced
488 those of microvertebrates, which are not found in TKSF. Thus, streams only acted as a
489 modification agent, as has been experimentally recorded by Thompson et al. (2011).

490 Only 9% of the analysed remains are affected by weathering and this only to a low degree,
491 suggesting that they were not at the mercy of the elements for long. Besides, biochemical
492 alterations are not substantial (5.79%), and trampling affected just 15.11% of the bones.
493 Finally, alterations due to carnivores such as tooth marks or furrowing on the epiphyses, which
494 would suggest access to carcasses prior to sedimentation, have not been observed. The
495 combination of these elements points to fast burial processes.

496 Fragmentation patterns show low incidence. More than 50% of the remains are over 4 cm in
497 size, and several long bones of large animals such as *Sivatherium* and buffalo have been
498 recorded. Furthermore, it has been observed that 65% of long bones have a diaphysis
499 circumference percentage higher than 50% (**Table 5**), and more than 69% of the remains show
500 diagenetic dry fractures (**Table 5**). Fractures with straight and mixed angles, close to 90°, have
501 been observed among these remains, as well as several fragments with transverse and
502 longitudinal transverse fractures. With regard to the bones with green fracture, 71,4% show
503 oblique planes, and 28.6% longitudinal plane with oblique angles.

504 The poor state of preservation, together with alterations such as abrasion and calcareous
505 concretions, hides the identification of anthropogenic alterations on bone surfaces (**Fig. 2d**).
506 Despite these determining factors, three cut marks could be identified on a large animal (size
507 5) rib fragment, another one on a 3b size hartebeest pelvis, and a further one on a 3b size

508 unguate metapodial. In this last specimen, however, marks are affected by polishing and
509 abrasion (**Fig. 3**). Finally, two impact flakes have been observed on a size 5 animal rib and on a
510 small size animal (size 2) diaphysis.

511 **4.2. Lithic taphonomy**

512 Crust which formed due to precipitation of calcium carbonate is present on 48.83 % of the
513 lithic pieces (567), and 16.10% (187) of pieces had sediment adhered to the surface.
514 Nevertheless, the degree of rounding could be analysed on the whole lithic series of TKSF
515 (1,154 items). Only 4.9% show light rounding and 1.1% intense roundness on the edges (**Table**
516 **7**). A third (51) of the pieces with some degree of rounding are shorter than 4 cm, and could
517 have been added by the sandy clay tuff that overlies the TKSF surface. This also suggests that
518 12 pieces between 4 and 10 cm long, and especially six pieces between 10 cm and 16 cm,
519 including a NQ and a VR handaxes, as well as a VR hammerstone, could be old pieces recycled
520 by hominins. Regarding raw materials, NQ show percentages slightly higher than VR (5% and
521 3.3% respectively), although this could be due to a lower representation of pieces shorter than
522 4 cm among the VR.

523 Over half (176; 51.6%) of the 341 flakes recorded at TKSF do not have fractures. Many of the
524 broken pieces (137; 40.2% of the whole), show small fractures that have not substantially
525 affected the original dimensions of the pieces, making the interpretation of the dorsal faces
526 possible (Rubio-Jara et al., 2017). Only 28 flakes (8.2 % of the whole) show substantial
527 fractures. On the other hand, the flakes are rarely affected by pseudo-retouch. This has only
528 been identified on three NQ pieces between 80 to 119 mm long and on a single VR piece.

529 **4.3. Orientation and fabric analysis**

530 Similar orientation patterns are evident for both artefacts and faunal remains in the TKSF level
531 (**Table 9**). The length of the mean vector, concentration, circular variance, and standard
532 deviation have analogous values, consistent with characteristics of isotropic populations (**Table**
533 **9, Fig. 4**). Furthermore, Rayleigh and Kuiper's tests results are consistent with an isotropic
534 distribution of the lithic industry ($Z = 1.488$, $p = 0.226$ and $V = 1.408$, $p = > 0.15$ by MBR and $Z =$
535 1.996 , $p = 0.136$ and $V = 1.682$, $p = 0.10 > p > 0.05$ by PMA) and faunal remains ($Z = 2.531$, $p =$
536 0.08 and $V = 1.438$, $p = > 0.15$ by MBR and $Z = 2.402$, $p = 0.091$ and $V = 1.485$, $p = > 0.15$ by
537 PMA).

538 The absence of items (such as natural clasts) susceptible to fabric analyses in this level, other
539 than artifacts and faunal remains, hinders the interpretation of the fabric results as a whole.
540 Some small differences are detected among the lithic industry and faunal fabric patterns. The
541 lithic industry is characterized by a lower girdle (girdle with cluster) degree than faunal remains
542 (**Table. 8, Fig. 5**), and a higher K index value in MBG ($K = 0.66$) than faunal remains ($K = 0.16$).
543 Likewise, the Vollmer's index values and F or CGI indexes also reinforce these small differences
544 in the fabric pattern (**Table. 8, Fig. 5**). Also, the eigenvalues of the lithic industry show a more
545 girdle fabric pattern ($S1 = S2 \gg S3$) than faunal remains, which show more lineal features ($S1$
546 $\gg S2 = S3$). Regardless, the stereogram plots show that both assemblages have an isotropic
547 feature (**Fig. 6**).

548 4.4. Spatial analysis

549 4.4.1. Density remains

550 The density and clustering analysis of the TKSF assemblage shows a significant degree of
551 density and clustering (**Table. 9; Fig. 7a**). Merging together all assemblages there are 27.82
552 items/m², with the nearest neighbour index ($R = 0.87$ $p = 0.000$) and Getis-Ord General G index
553 ($G = 0.00$ $p = 0.000$) coincident with a large degree of clustering (**Table. 9**).

554 The lithic industry shows a larger density value (21.08 items/m²) than bones (6.02 items/m²),
555 but the degree of clustering is similarly high for both types of items and of similar value. The
556 Getis-Ord General G index is also similar and shows higher cluster values for the lithic industry
557 than for the faunal remains (**Table. 9; Fig. 7b-c**).

558 As can be observed in the density maps, the largest concentrations of lithic and bones do not
559 overlap (**Fig. 7b-c**). However, in the south-eastern area of the excavation surface, a large
560 concentration of lithics close to the main accumulation of long bones is visible. The faunal
561 concentration produces a conspicuous semi-circular shape that surrounds the centre and
562 largest accumulation of lithic implements. The largest accumulation of bones defines an
563 external position with regard to this accumulation of artefacts (**Fig. 7b-c**).

564 The density and clustering analyses applied to the main techno-typological categories show
565 the highest densities for shatter and flakes (10.79 and 6.80 items/m², respectively), as well as
566 the highest degree of cluster (**Table 10**). Cobbles, percussion material, and LCTs show lower
567 densities, with values around 1 item/m². Also, the degree of clustering and the neighbouring
568 index are also substantially lower, both of which show a random or dispersed pattern (**Table**
569 **10**). In the density maps, it can be observed that cobbles, percussion materials, cores, and LCTs
570 are located near the largest accumulation of faunal remains (**Fig. 8**). This situation seems to
571 define a specific area of activity in the vicinity of the main faunal accumulation, which is
572 suggestive of hominin activity.

573 4.4.2. Distribution pattern

574 The results of the distribution pattern analysis at TKSF show a specific association related to
575 the density features mentioned above. Groups of K means occur in large numbers and define
576 some specific concentrations of large faunal remains and artifacts with geo-statistical
577 significance (**Fig.9**). The Cluster Outliers and Hot Spots maps similarly show a more patterned
578 distribution with local concentrations (**Fig. 10-11**).

579 4.4.3. Spatial point patterns

580 The quadrat chi-square test showed that bones ($X^2=334.30$; $p=0.0195$) and lithics ($X^2=454.76$;
581 $p=0.0198$) at TKSF were distributed in a significantly different manner from a stationary
582 pattern. The DCLF test showed that the distribution of bones ($u=108704$; $p=0.01$) and lithics
583 ($u=24015$; $p= 0.01$) followed an inhomogeneous pattern. This is also evidenced when
584 comparing inhomogeneous Poisson simulation to the TKSF bone and lithic spatial patterns (**Fig.**
585 **12**). When using the homogeneous version of the L-function, one gets the impression that
586 both lithics and bones show a clustering trend (**Fig. 13A, 13B**). However, when using the
587 inhomogeneous L-function, it can be clearly noticed that lithics and bones follow a fairly
588 inhomogeneous pattern (**Fig. 13C, 13D**). The point pattern of the bones shows a trend towards

589 clustering after a radius of 1500 mm, which indicates that in a radius of 1500 mm of any
590 randomly chosen bone, other bones tend to cluster instead of using complete spatial
591 randomness, and that lithics are more scattered than bones. This can be clearly observed in
592 the kernel density maps of bones and lithics (**Fig. 14**). Bones show a more concentrated
593 pattern, with one hot spot area, as shown by the adaptive density map, situated more distally
594 than the hotter zone of lithic concentration (**Fig. 14**). Although there is an overlap of high
595 intensity areas, showing co-dependence of spatial marks (i.e. bones and lithics) (see below),
596 the different location of the hot spots indicates that this co-dependence is not very strong, as
597 suggested by the random labelling J-dot function (**Fig. 15**).

598 Clark-Evans tests show that bones ($R=0.85$; $p=0.006$) and lithics ($R=0.86$; $p=0.005$) are
599 clustered, which suggests inter-point dependence in their spatial distribution. However, this is
600 the artificial result of the test, which is dependent on the homogeneity of the point process.
601 Given that the TKSF pattern is inhomogeneous, a Hopkins-Skellam test on bones ($A=0.20$;
602 $p<0.000$) and lithics ($A=0.13$; $p<0.000$) shows that clustering is not documented and that the
603 data fit an inhomogeneous Poisson pattern well.

604 Cross-type analysis shows a trend towards slight clustering in bones starting at a distance of
605 one meter from any random point and an increasing trend of slight and progressive clustering
606 in lithics starting at radii of half a meter from any random point. The off-diagonal L_{ij} graphs
607 indicate an increasing co-dependence in the form of clustering of lithic and bones after a
608 radius of 20 cm of any random point (**Fig. 16**). This suggests that a) the deposition of bones and
609 stone tools are spatially dependent, b) this spatial dependence has been maintained despite
610 postdepositional biostratigraphic taphonomic processes and, c) such a spatial co-dependence
611 indicates a functional link between stone tools and bones during site formation. This pattern is
612 even more nuanced, however, because two distinctive activity areas are documented for
613 lithics and bones, both of which could have been created through the independent or
614 combined action of either post-depositional processes and/or activities that required tools for
615 tasks other than carcass butchery (**Fig. 14 C, D**). This is further supported by the random
616 labelling method, which shows that if this spatial co-dependence can be observed, it is not as
617 strong as to be spatially concurrent, which would be the case if random labelling displayed the
618 TKSF point process outside the boundaries of the confidence interval for a random distribution
619 (**Fig. 15**).

620 **5. Discussion**

621 Knowledge of the Acheulean in East Africa has developed substantially in the last decades.
622 (Kuman and Clarke, 2000; Quade et al., 2004; Texier, 2005; Kuman, 2007; Beyene et al., 2013;
623 Gallotti, 2013; Brown and McDougall, 2011; de la Torre, 2011; Domínguez-Rodrigo et al., 2013;
624 Díez-Martín et al., 2014; Gibbon et al., 2014; Santonja et al., 2014; Díez-Martín et al., 2015; de
625 la Torre et al., 2018; Gallotti and Mussi, 2018). A difference between the sites older than 1.2
626 Ma and those younger than 1 Ma has been proposed based on analyses of the technological
627 strategies implemented on the manufacturing of lithic tools (de la Torre and Mora, 2005;
628 Sharon, 2007; 2010; Stout, 2011; Díez-Martín and Eren, 2012; Beyene et al., 2013; Sahnouni et
629 al., 2013; Gallotti, 2013; Gallotti and Mussi, 2017; 2018; Texier, 2018). Thus, sites older than
630 1.2 Ma are considered as early Acheulean. Our proposal is to use this appellation with a
631 chronological sense, considering new data from FLK West~1.69 Ma (Díez-Martín et al., 2015)

632 and TK-1.33 Ma (Santonja et al. 2014; 2018; Rubio-Jara et al. 2017), where complex processes in
633 handaxe configuration have been described. In order to understand the identity of the first
634 Acheulean sites, the variables that have influenced the selection of those strategies must be
635 discriminated, and the functionality of the sites must be seen as a determinant conditioner of
636 this process (Presnyakova et al., 2018).

637 A good deal of early Acheulean sites are either located in fluvial environments or have suffered
638 other important post-depositional processes (Domínguez-Rodrigo et al., 2009; Gibbon et al.,
639 2009; Gallotti, 2013; Diez-Martín et al., 2014; Uribelarrea et al., 2017; de la Torre et al., 2018;
640 Semaw et al., 2018), which will have an influence on the analysis of these sites' functionality.
641 Because the spatial relationships of the different elements of the archaeological assemblage
642 are not significantly altered, the association of these elements must be analysed, particularly in
643 the cases in which the remains are so badly preserved that taphonomic analyses cannot be
644 carried out.

645 The densest known concentration of early Acheulean sites has been recorded in Bed II at
646 Olduvai Gorge (Leakey, 1971; Santonja et al., 2014; Diez-Martín et al., 2009; 2014; 2015;
647 Sánchez-Yustos et al., 2016; Rubio-Jara et al., 2017; de la Torre et al., 2018). Among the
648 Olduvai early Acheulean sites, the particular features of the lithic assemblages and
649 sedimentary environments identified in TK offer great potential for analysing the influence of
650 functionality on the variability of the technological strategies during the early Acheulean
651 stages. Two Acheulean paleosurfaces were identified at TK, TKLF and TKSF, with no significant
652 temporal diachrony, although with substantial differences between their archaeological
653 assemblages (Rubio-Jara et al., 2017).

654 The analysis of the lithic industry has shown higher density in TKLF than in TKSF (38.4 and 12.1
655 items per m² respectively). It has allowed the discernment of a differentiated economy of tool
656 manufacturing: at TKLF, debitage of NQ and VR was transformed on site, whereas in TKSF only
657 the NQ cores were knapped, and VR cores were flaked, at least in part, outside the site. Bipolar
658 and freehand percussion are better represented in TKSF than in TKLF, and opportunistically
659 exploited cores are more frequent in TKLF. Discoid and bifacial discoid cores dominate in TKSF,
660 whereas flakes with rectangular formats prevail in TKSF. However, the greatest differences
661 have been observed among the handaxes: 85 pieces in TKLF and 53 items in TKSF (Rubio-Jara
662 et al. 2017; Santonja et al. 2018). In TKSF items heavier than 1 kg and longer than 19 cm are
663 rare, whereas in TKLF items >19 cm and, on occasion, as heavy as 3 kg, were dominant. In the
664 TKLF pieces, the functional area is concentrated on the apical third and they have backs on the
665 base or on the edges. However, in TKSF, the whole perimeter is the cutting edge, and points
666 and edges are more rejuvenated in TKSF than in TKLF.

667 From the point of view of lithic taphonomy, the degree of rounding at TKSF is very low and
668 affects mainly pieces shorter than 4 cm, which were possibly redeposited by the sandy clay tuff
669 that overlies this surface. However, six pieces between 10 and 16 cm that show some
670 rounding, including two handaxes and a VR hammerstone, could have been recycled by
671 hominins for later use from other deposits. The high flake fracture indexes are consistent with
672 the knapping of NQ, which breaks easily, and therefore cannot be blamed on substantial post-
673 depositional processes, as is suggested by the low number of flakes with pseudo-retouch.
674 Nevertheless, a certain degree of trampling cannot be ruled out.

675 The faunal analysis of TKLF reveals a high MNI (i.e. 47), in which suids, antilopines and
676 especially equids and alcelaphines dominate, and tragelaphines, bovines, reduncines, hippos,
677 and crocodiles are present in lower frequencies (Hill, 1983; Egeland, 2008; Egeland and
678 Domínguez-Rodrigo, 2008; Yravedra et al., 2016). Only 248 pieces, 23% of the whole, show
679 good preservation. The presence of green fractures (in 99 pieces) in small and medium-sized
680 animal, a single percussion mark (on a tibial shaft from a medium-sized one), one boring in a
681 hippopotamus jaw (Hill, 1983), and a few tooth marks (4), indicate hominin and, to a lesser
682 extent, carnivore activity (Yravedra et al., 2016). The analysis of the bones' cortical surfaces
683 points to prolonged subaerial exposure and the influence of overland water flow and other
684 erosive agents before being buried (Yravedra et al., 2016).

685 This scene is quite different to that observed in TKSF, where almost a third of the bone
686 remains in which sizes were identified belong to species between 750 kg and 2,000 kg, and
687 more than another third were species heavier than 2,000 kg. Some remains of elephant and
688 buffalo have been identified, although *Sivatherium* and hippopotamus are dominant.
689 Substantial differences are identified according to the elements represented: whereas in
690 *Sivatherium* axial and appendicular elements dominate, dental fragments, lower appendicular
691 bones and metapodials are most common for hippos, which suggests that these mega
692 herbivores were fully represented on site. The low frequency of small and medium-sized
693 mammals does not allow the establishment of conclusions regarding representation profiles.
694 Despite evidence of concretion and altered cortical surfaces on 68% of the remains, five
695 anthropogenic bones have been recorded: cut marks were observed on a size 5 animal rib and
696 also on two size 3b bones. Two impact flakes were observed as well, one of them also on a size
697 5 animal rib. Weathering, trampling, and biochemical alterations suggest rapid burial.

698 Taphonomic analysis of the lithic industry and the faunal remains of TKSF is compatible with
699 the absence of post-depositional processes that could have substantially modified the original
700 spatial relationships of lithic pieces and bones. In addition, the lithic industry and faunal
701 remains show orientation patterns consistent with an isotropic distribution. With regard to
702 fabric analysis, the lithic industry shows a more girdle fabric, while bones display a more linear
703 fabric pattern. However, the stereogram plots show that both assemblages have an isotropic
704 feature, and the aforementioned differences can be related to the large metric differences
705 between the lithics and faunal remains, where the presence of many large bones can be a
706 problem in establishing solid comparisons between both assemblages.

707 Therefore, TKSF relates to a paleosurface in which the archaeological assemblage is found in
708 an autochthonous position with no significant spatial modifications and that was subject to a
709 relatively fast burial process that allows the analysis of its functionality. Site functionality is in
710 fact being explored through biomarker analysis and use-wear analysis of the entire
711 assemblages of knapped lithic pieces-a first for an Acheulean site- (Bello-Alonso et al., 2016,
712 2018). The faunal remains indicate an assemblage of megaherbivores, among which are
713 several complete *Sivatherium* bones. No evidence for carnivore modification is present and
714 very few bones are green-broken. Consequently, it seems that human intervention on the
715 fauna was not intensive, although it has been confirmed by the presence of cut marks on size 5
716 and 3b animals. However, considering that in more than two thirds of the faunal remains
717 cortical analysis could not be carried out, geo-statistical analysis has been implemented in
718 order to establish dependency relationships between the fauna and lithic industry.

719 The spatial pattern analyses show a significant density and clustering degree; however, the
720 lithic industry displays larger density values and higher cluster values than bones. In relation to
721 techno-typological categories, shatter and flakes show the highest densities and cluster
722 degrees. The largest concentrations of lithics and bones do not overlap; nevertheless, the main
723 accumulation of long bones occurs in the south-eastern area, where a semi-circular shape of
724 long bones surrounding the central and largest accumulation of knapped stones is displayed.
725 Most of the *Sivatherium* bones and other remains with sizes compatible with this animal are
726 also in this area. Furthermore, in this sector, the density maps show clusters of percussion
727 elements, cobbles that could also have been used as hammerstones, and LCTs. In addition, two
728 of the three bones with percussion marks and one of the three bones with cut marks, as well
729 as several others with green fractures, were identified in this area.

730 According to spatial point patterns analyses, point statistical properties of the TKSF bones and
731 lithics do not depend on location, follow a spatially dependent pattern, and lithics are more
732 scattered than bones. This suggests the presence of one hot spot area. The cross-type analysis
733 suggests that the deposition of bones and stones are spatially-dependent, which indicates a
734 functional link between them during site formation. However the random labelling method
735 shows that this co-dependence is not as strong as to be spatially concurrent, because of post-
736 depositional processes and/or stone tools being used in activities other than carcass butchery.
737 As the taphonomic analysis of lithics and bones rules out the first scenario, the results suggest
738 the second is more probable.

739 **6. Conclusions**

740 In order to understand the identity of the early Acheulean, it is necessary to discriminate
741 between the variables that influenced the selection of technological strategies, and here
742 functionality is a determinant conditioner. To reach this goal, first of all, it is necessary to
743 analyze the spatial relationships of the different elements of the archaeological assemblage
744 and the associations among these elements.

745 As TK two main paleosurfaces, TKLF and TKSF, have no significant temporal diachrony but
746 there are substantial differences between their archaeological assemblages. The TK site thus
747 offers much potential to assess the influence of functionality in the variability of the
748 technological strategies during the early Acheulean.

749 In this paper we have assessed functionality at TKSF through lithic, faunal, taphonomic, and
750 spatial analyses. Taphonomic data, orientation patterns, and fabric analyses rule out significant
751 post-depositional processes that could have modified the spatial relationships between lithics
752 and faunal remains. TKSF relates to a paleosurface in which the archaeological assemblage is
753 found in autochthonous position and experienced a relatively rapid process of burial that
754 allows the analysis of its functionality. In the absence of the results of wear use and biomarker
755 analyses, among others, human activities on macromammals have been evaluated with the
756 available data.

757 The bone remains seem to indicate an assemblage of megaherbivores, among which are several
758 complete *Sivatherium* bones. No evidence for carnivore intervention was found, green
759 fractures are rare, and only a few cut marks on size 5 and 3b animals have been identified.
760 Hence, it seems that human intervention on the fauna was not intensive, although it should be

761 taken into consideration that more than two thirds of the bones show poor cortical
762 preservation.

763 Spatial and geostatistical analyses suggest a functional link between the lithics and bones
764 during site formation, but this co-dependence is not as strong as to be spatially concurrent, as
765 stone tools were used in more activities other than carcass butchery. Most of the *Sivatherium*
766 bones were located in the south-eastern spot of the excavated area, where a semi-circular
767 shape of long bones surrounding the central and largest accumulation of knapped stones was
768 displayed, with clusters of percussion elements, cobbles, and LCTs, as well as bones with
769 percussion and cut marks and green fractures.

770 Therefore, in the TKSF analysed paleosurface, activities related to megaherbivore processing
771 were carried out, mainly in the south-eastern area, where the main accumulation of long
772 bones were located, especially *Sivatherium*, together with clusters of percussion elements,
773 cobbles, and LCTs, and most of the bones showed percussion, cut marks, and green fractures.
774 The wide dispersion of flakes and shatter indicates that other human activities unrelated to the
775 processing of animals were also carried out on this surface. We are currently trying to
776 understand such activities through use-wear and biomarker analyses on stone tools.

777 The TKLF paleosurface, only 20-40 cm below TKSF, shows a very different scenario; as it took
778 much longer to be buried, the find density of the lithic industry is considerably higher, and the
779 preservation of the bone surface is poorer. The large taxonomic diversity, with no cut marks
780 and only one percussion mark, can be interpreted as the result of natural processes, so the
781 main anthropogenic input could be related to other resources where large handaxes were
782 necessary. The technological and techno-economic study reveals strong differences between
783 the lithic industry in TKLF and TKSF, especially among the handaxe configuration. Without
784 assessment of site functionality and chronological context, this data could have led to the
785 differences observed at TKLF and TKSF being assigned to different Acheulean stages.

786

787

788 **Acknowledgements.**

789 We thank the Tanzanian Commission for Science and Technology (COSTECH), the Department
790 of Antiquities and Ngorongoro Conservation Area Authority in the Ministry of Natural
791 Resources and Tourism for permission to conduct research at Olduvai Gorge; the Spanish
792 Ministry of Science and Technology (HAR2010-18952-C02-01; HAR2013-45246-C3-2-P;
793 HAR2017-82463-C4-2-P Projects) and to the Comunidad de Madrid, which Funded this
794 research through its research and development programmes (S2010/BMD-2330 R+D Project).
795 EMQ was funded by a Xunta de Galicia Post-Doc Grant. We are also grateful to Raquel Rojas
796 Mendoza for restoration of the faunal remains, and Marta Muñiz and Ciara Travers for the
797 English editing. Finally, we would like to thank especially the anonymous reviewers for their
798 comments and suggestions, and also the guest editor Charles Egeland for his exhaustive and
799 careful edition of the text, which has greatly contributed to improve the final result.

800

801 **References**

- 802 Andrefsky, W. 2005, *Lithics: Macroscopic approaches to analysis*. Cambridge University Press, Cambridge,
803 321 pp.
- 804 Baddeley, A., Rubak, E., Turner, R. 2015. *Spatial Point Patterns: Methodology and Applications with R*. CRC
805 Press, London, 848 pp.
- 806 Barone, R., 1976. *Anatomie comparée des mamifères domestiques: Ostéologie*. Vigot Frères, Paris.
- 807 Behrensmeyer, A.K., 1978. Taphonomic and ecologic information from bone weathering. *Paleobiology* 4,
808 150-162.
- 809 Bello-Alonso, P., Ríos-Garaizar, J., Panera, J., Pérez-González, A., Rubio-Jara, S., Rojas-Mendoza, R.,
810 Domínguez-Rodrigo, M., Baquedano, E., Santonja, M. (submitted). A use-wear interpretation of the
811 most common raw materials from the Olduvai Gorge: Naibor Soit quartzite. *Quaternary*
812 *International*.
- 813 Bello-Alonso, P., Ríos-Garaizar, J., Santonja, M., Panera, J. 2016: Approach to economic activities developed
814 in the African Acheulean. Use-wear analysis from Thiongo Korongo site (Olduvai Gorge, Tanzania).
815 Poster, 23rd Biennial meeting of the Society of Africanist Archaeologists, Toulouse, France.
- 816 Bello-Alonso, P., Ríos-Garaizar, J., Santonja, M., Panera, J., Rubio-Jara, S., Rojas, R., Pérez-González, A., 2018.
817 First experimental study with basalt for the use-wear analysis of Acheulean lithic industry of Thiongo
818 Korongo site (Olduvai Gorge, Tanzania). Poster 2^o meeting AWRANA, Nice, France.
- 819 Bertran, P., Texier, J.-P., 1995. Fabric Analysis: Application to Paleolithic Sites. *Journal of Archaeological*
820 *Science* 22, 521-535. Doi.org/10.1006/jasc.1995.0050.
- 821 Beyene, Y., Katoh, S., WoldeGabriel, G., Hart, W. K., Uto, K., Sudo, M., Kondo, M., Hyodo, M., Renne, P.R.,
822 Suwa, G., Asfaw, B., 2013. The characteristics and chronology of the earliest Acheulean at Konso,
823 Ethiopia. *Proceedings of the National Academy of Sciences* 110, 1584–1591.
- 824 Binford, L.R., 1978. *Nunamiut ethnoarchaeology*. New York. Academic Press.
- 825 Bivand, R., 2010. Exploratory spatial data analysis. In: Fischer, M., Getis, A., (Eds.). *Handbook of Applied*
826 *Spatial Analysis*. Springer, Berlin, 219-254
- 827 Blumenschine, R.J., 1988. An experimental model of the timing of hominid and carnivore influence on
828 archaeological bone assemblages. *Journal of Archaeological Science* 15, 483-502.
- 829 Capaldo, D., Blumenschine, R.J., 1994. A quantitative diagnosis of notches made by hammerstone
830 percussion and Carnivore Gnawing on bovid long bones, *American Antiquity* 59 (4), 724-748.
- 831 Blumenschine, R.J., 1995. Percussion marks, tooth marks, and experimental determinations of the timing of
832 hominid and carnivore access to long bones at FLK Zinjanthropus, Olduvai Gorge, Tanzania. *Journal of*
833 *Human Evolution* 29, 21-51.
- 834 Blumenschine, R.J., Selvaggio, M.M., 1988. Percussion marks on bone surfaces as a new diagnostic of
835 hominid behaviour. *Nature* 333, 763-765.
- 836 Boots, B., Getis, A., 1988. *Point Pattern Analysis*. Sage University, Newcastle.
- 837 Bower, J.R.F., 1977. Attributes of Oldowan and Lower Acheulean tools: “tradition” and design in the Early
838 Lower Palaeolithic. *The South African Archaeological Bulletin* 32, 113-126.

- 839 Brain, C.K., 1969. The contribution of Namib Desert Hottentots to an understanding of australopithecine
840 bone accumulations. *Scientific Papers of the Namib Desert Research Station* 39, 13-22.
- 841 Brown, F.H., McDougall, I., 2011. Geochronology of the Turkana depression of northern Kenya and
842 southern Ethiopia. *Evolutionary anthropology* 20, 217-227.
- 843 Bunn, H.T., 1982. Meat-eating and Human Evolution: Studies on the Diet and Subsistence Patterns of Plio-
844 pleistocene Hominins in East Africa (Ph. dissertation). University of California, Berkeley.
- 845 Burroni, D., Donahue, R. E., Pollard, A. M., 2002. The surface alteration features of flint artefacts as a record
846 of environmental processes. *Journal of Archaeological Science* 29 (11), 1277–1287. <https://doi.org/10.1006/jasc.2001.0771>.
- 848 Bustos-Pérez, G., Díaz, S., Baena, J., 2019. An Experimental Approach to Degrees of Rounding Among Lithic
849 Artifacts. *Journal of Archaeological Method and Theory*, 1-33.
- 850 Capaldo, S.D., Blumenshine, R.J., 1994. A quantitative diagnosis of notches made by hammerstone
851 percussion and carnivore gnawing on bovid long bones. *American Antiquity* 59, 724-748.
- 852 Clark, J. D., Kurashina, H., 1979. Hominid occupation of the east-central highlands of Ethiopia in the Plio-
853 Pleistocene. *Nature* 282, 33–39.
- 854 Cobo-Sánchez, L., Aramendi, J., Domínguez-Rodrigo, M., 2014. Orientation patterns of wildebeest bones on
855 the lake Masek floodplain (Serengeti, Tanzania) and their relevance to interpret anisotropy in the
856 Olduvai lacustrine floodplain. *Quaternary International* 322-323, 277-284.
857 [Doi.org/10.1016/j.quaint.2013.07.130](https://doi.org/10.1016/j.quaint.2013.07.130).
- 858 Deino, A., Domínguez-Rodrigo, M., Luque, L., 2006. $^{40}\text{Ar}/^{39}\text{Ar}$ dating of the Pleistocene Peninj Group, Lake
859 Natron, Tanzania. *Eos Trans. AGU*, 87 (52), Fall Meeting. Supplement, Abstracts, C1771.
- 860 Dibble, H., Chase, P. G., McPherron, S. P., Tuffreau, A., 1997. Testing the reality of a “living floor” with
861 archaeological data. *American Antiquity* 62, 629–651.
- 862 Diez-Martin, F., Eren, M. I., 2012. The Early Acheulean in Africa: past paradigms, current ideas, and future
863 directions. In: Domínguez-Rodrigo, M. (Ed.). *Stone Tools and Fossil Bones: Debates in the*
864 *Archaeology of Human Origins*. Cambridge University, pp.310-357.
- 865 Diez-Martín, F., Sánchez-Yustos, P., Domínguez-Rodrigo, M., Mabulla, A., Barba, R., 2009. Were Olduvai
866 hominins making butchering tools or battering tools? Analysis of a recently excavated lithic
867 assemblage from BK (Bed II, Olduvai Gorge, Tanzania). *Journal of Anthropological Archaeology* 28 (3),
868 274-289.
- 869 Diez-Martín, F., Sánchez Yustos, P., Domínguez-Rodrigo, M., Prendergast, M.E., 2011. An experimental
870 study of bipolar and freehand knapping of Naibor Soit quartz from Olduvai Gorge (Tanzania).
871 *American Antiquity* 76, 690-708.
- 872 Diez-Martín, F., Sánchez-Yustos, P., de Luque, L., 2018. The East African Early Acheulean of Peninj (Lake
873 Natron, Tanzania). In Gallotti, R., Mussi, M., 2018 (Eds). *The Emergence of the Acheulean in East*
874 *Africa and Beyond*. Springer, Cham, pp. 129-151.
- 875 Diez-Martín, F., Sánchez Yustos, P., UribeArrea, D., Baquedano, E., Mark, D.F., Mabulla, A., Fraile, C.,
876 Duque, J., Díaz, I., Pérez-González, A., Yravedra, J., Egeland, C.P., Organista, E., Domínguez-Rodrigo,
877 M., 2015. The Origin of the Acheulean: The 1.7 Million-Year-Old Site of FLK West, Olduvai Gorge
878 (Tanzania). *Scientific Reports* 5, 17839.

- 879 Diez-Martín, F., Sánchez-Yustos, P., UribeArrea, D., Domínguez-Rodrigo, M., Fraile-Márquez, C., Obregón, R.
880 A., Bunn, H. T., 2014. New archaeological and geological research at SHK main site (Bed II, Olduvai
881 Gorge, Tanzania). *Quaternary international*, 322, 107-128.
- 882 Domínguez-Rodrigo, M., Alcalá, L., Luque, L., 2009. *Peninj: A research project on human origins 1995-2005*.
883 Oxbow Books.
- 884 Domínguez-Rodrigo, M., Bunn, H.T., Pickering, T.R., Mabulla, A.Z.P., Musiba, C.M., Baquedano, E., Ashley,
885 G.M., Diez-Martin, F., Santonja, M., UribeArrea, D., Barba, R., Yravedra, J., Barboni, D., Arriaza, C.,
886 Gidna, A., 2012. Autochthony and orientation patterns in Olduvai Bed I: a re-examination of the
887 status of post-depositional biasing of archaeological assemblages from FLK North (FLKN). *Jornal of*
888 *Archaeological Science* 39, 2116-2127. Doi.org/10.1016/j.jas.2012.02.027
- 889 Domínguez-Rodrigo, M., Cobo-Sánchez, L., 2017. A spatial analysis of stone tools and fossil bones at FLK Zinj
890 22 and PTK I (Bed I, Olduvai Gorge, Tanzania) and its bearing on the social organization of early
891 humans. *Palaeogeography, Palaeoclimatology, Palaeoecology* 488, 21-34.
- 892 Domínguez-Rodrigo, M., Cobo-Sánchez, L., Yravedra, J., UribeArrea, D., Arriaza, C., Organista, E.,
893 Baquedano, E., 2017. Fluvial spatial taphonomy: a new method for the study of post-depositional
894 processes. *Archaeological and Anthropological Sciences*, 1–21.
- 895 Domínguez-Rodrigo, M., de Juana, S., Galán, A.B., Rodríguez, M., 2009. A new protocol to differentiate
896 trampling marks from butchery cut marks. *Journal of Archaeological Science* 36, 2643-2654.
- 897 Domínguez-Rodrigo, M., Martínez-Navarro, B., 2012. Taphonomic analysis of the early Pleistocene (2.4 Ma)
898 faunal assemblage from A.L. 894 (Hadar, Ethiopia). *Journal of Human Evolution* 62, 315-327.
- 899 Domínguez-Rodrigo, M., Pickering, T. R., Baquedano, E., Mabulla, A., Mark, D. F. Musiba, C., Bunn, H. T.,
900 UribeArrea, D., Smith, V., Diez-Martin, F., Pérez-González, A., Sánchez, P., Santonja, M., Barboni, D.,
901 Gidna, A., Ashley, G., Yravedra, J., Heaton, J. L., Arriaza M.C., 2013. First Partial Skeleton of a 1.34-
902 Million-Year-Old Paranthropus boisei from Bed II, Olduvai Gorge, Tanzania. *PLoS ONE* 8, e80347.
903 doi:10.1371/journal.pone.0080347.
- 904 Domínguez-Rodrigo, M., UribeArrea, D., Santonja, M., Bunn, H.T., García-Pérez, A., Pérez-González, A.,
905 Panera, J., Rubio-Jara, S., Mabulla, A., Baquedano, E., Yravedra, J., Diez-Martín, F., 2014.
906 Autochthonous anisotropy of archaeological materials by the action of water: experimental and
907 archaeological reassessment of the orientation patterns at the Olduvai sites. *Jornal of*
908 *Archaeological Science* 41, 44-68. Doi.org/10.1016/j.jas.2013.07.025
- 909 Dorman, M. 2014. *Learning R for Geospatial Analysis*. Packt Publishing Ltd, London, 360 pp.
- 910 Dray, S., Pélissier, R., Couteron, P., Fortin, M.-J., Legendre, P., Peres-Neto, P.R., Bellier, E., Bivand, R.,
911 Blanchet, F.G., De Cáceres, M., et al., 2012. Community ecology in the age of multivariate multiscale
912 spatial analysis. *Ecological Monographs* 82 (3), 257–275.
- 913 Egeland, C.P., 2008. Patterns of early hominid site use at Olduvai Gorge. *Mitteilungen der Gesellschaft für*
914 *Urgeschichte* 17, 9-37.
- 915 Egeland, C.P., Domínguez-Rodrigo, M., 2008. Taphonomic perspectives on hominin site use and foraging
916 strategies during the Bed II times at Olduvai Gorge, Tanzania. *Journal of Human Evolution* 55, 1031-
917 1052.
- 918 Fisher, N.I., 1993. *Statistical Analysis of Circular Data*. Cambridge University Press.

- 919 Gallotti, R., 2013. An older origin for the Acheulean at Melka Kunture (Upper Awash, Ethiopia): techno-
920 economic behaviours at Garba IVD. *Journal of Human Evolution* 65(5), 594-620.
- 921 Gallotti, R., Mussi, M., 2017. Two Acheuleans, two humankinds: From 1.5 to 0.85 Ma at Melka Kunture
922 (Upper Awash, Ethiopian highlands). *Journal of Anthropological Sciences* 95, 1-46.
- 923 Gallotti, R., Mussi, M., 2018. Before, During, and After the Early Acheulean at Melka Kunture (Upper Awash,
924 Ethiopia): A Techno-economic Comparative Analysis. In Gallotti, R., Mussi, M., 2018 (Eds). *The*
925 *Emergence of the Acheulean in East Africa and Beyond. Contributions in Honor of Jean Chavaillon.*
926 *Vertebrate Paleobiology and Paleoanthropology Series.* Springer, Cham, pp. 53-92.
- 927 García-Moreno, A., Smith, G.M., Kindler, L., Pop, E., Roebroeks, W., Gaudzinski-Windheuser, S., Klinkenberg,
928 V., 2016. Evaluating the incidence of hydrological processes during site formation through
929 orientation analysis. A case study of the middle Palaeolithic Lakeland site of Neumark-Nord 2
930 (Germany). *Journal of Archaeological Sciences. Reports* 6, 82-93. 10.1016/j.jasrep.2016.01.023
- 931 Gentry, A.W., Gentry, A., 1978. Fossil Bovidae (Mammalia) of Olduvai Gorge, Tanzania. Part 1. *Bulletin of*
932 *the British Museum (Natural History). Geology Series*, vol. 29, pp. 289-446.
- 933 Gentry, A.W., Gentry, A., 1978a. Fossil Bovidae (Mammalia) of Olduvai Gorge, Tanzania. Part 2. *Bulletin of*
934 *the British Museum (Natural History). Geology Series*, vol. 30, pp. 1-83.
- 935 Getis, A., Ord, J.K., 1992. The analysis of spatial association by use of distance statistics. *Geographical*
936 *Analysis* 24, 189-206.
- 937 Gibbon, R. J., Granger, D. E., Kuman, K., Partridge, T. C., 2009. Early Acheulean technology in the Rietputs
938 Formation, South Africa, dated with cosmogenic nuclides. *Journal of Human Evolution* 56 (2), 152-
939 160.
- 940 Gibbon, R. J., Pickering, T. R., Sutton, M. B., Heaton, J. L., Kuman, K., Clarke, R. J., Brain, C.K., Granger, D. E.,
941 2014. Cosmogenic nuclide burial dating of hominin-bearing Pleistocene cave deposits at Swartkrans,
942 South Africa. *Quaternary Geochronology* 24, 10-15.
- 943 Giusti, D., Turloukis, V., Konidaris, G., Thompson, N., Karkanas, P., Panagopoulou, E., Harvati, K., 2018.
944 Beyond maps: Patterns of formation processes at the Middle Pleistocene open-air site of Marathousa
945 1, Megalopolis basin, Greece. *Quaternary International* 497, 137-153
946 doi.org/10.1016/j.quaint.2018.01.041.
- 947 Glauberman, P. J., Thorson, R. M., 2012. Flint patina as an aspect of “flaked stone taphonomy”: a case study
948 from the loess terrain of the Netherlands and Belgium. *Journal of Taphonomy* 10 (1), 21-43.
- 949 Harding, P., Gibbard, P. L., Lewin, J., Macklin, M. G., Moss, E. H., 1987. The transport and abrasion of flint
950 handaxes in a gravel-bed river. In: Sieveking, G., Newcomer, M. (Eds.), *The human uses of flint and*
951 *chert: proceedings of the fourth international flint symposium held at Brighton Polytechnic.*
952 Cambridge: Cambridge University Press, pp. 115–126.
- 953 Hay, R., 1976. *Geology of the Olduvai Gorge.* University of California Press, Berkeley, p. 203.
- 954 Hay, R., 1994. Geology and dating of Beds III, IV, and the Masek Beds. In: Leakey, M. D., Roe, D.A. (Eds.),
955 *Olduvai Gorge Excavations in Beds III, IV, and the Masek Beds 1968–1971* Cambridge: Cambridge
956 University Press, pp.8-14.
- 957 Herzlinger, G., Pinsky, S., Goren-Inbar, N., 2015. A note on handaxe knapping products and their breakage
958 taphonomy: An experimental view. *Journal of Lithic Studies* 2 (1), 65-82.

- 959 Hill, A., 1983. Hippopotamus Butchery by *Homo erectus* at Olduvai. *Journal of Archaeological Science* 10,
960 135-137.
- 961 Hiscock, P., 2002. Quantifying the size of artefact assemblages. *Journal of Archaeological Science* 29 (3),
962 251-258.
- 963 Hodder, I., Orton, C., 1976. *Spatial analysis in archaeology*. Serie: *New Studies in Archaeology*. Cambridge
964 University Press.
- 965 Hosfield, R. T., 2011. Rolling stones: understanding river-rolled Paleolithic artifact assemblages. In: Brown,
966 A., Basell, L., Butzer, K. (Eds.). *Geoarchaeology, climate change, and sustainability The Geological*
967 *Society of America Special Paper 476*, 37–52.
- 968 Hosfield, R. T., Chambers, J. C., 2003. Flake modifications during fluvial transportation: three cautionary
969 tales. *Lithics* 24, 57–65.
- 970 Isaac, G. L., Curtis, G. H., 1974. Age of early Acheulian industries from the Peninj Group, Tanzania. *Nature*
971 249, 624–6627.
- 972 Jones, P.R., 1994. Results of experimental work in relation to the stone industries of Olduvai Gorge. In:
973 Leakey, M. (Ed.), *Olduvai Gorge. 5. Excavations in Beds III, IV and the Masek Beds, 1968-1979*,
974 Cambridge University Press, Cambridge, pp. 254-298.
- 975 Kimura, Y., 2002. Examining time trends in the Oldowan technology at Beds I and II, Olduvai Gorge. *Journal*
976 *of Human Evolution* 43, 291-321.
- 977 Kuman, K., 2007. The Earlier Stone Age in South Africa: site context and the influence of cave studies. In:
978 Pickeirng, T.R., Schick, K., Toth, N. (Eds.), *Breathing life into fossils: Taphonomic studies in Honour of*
979 *CK (Bob) Brain*. Stone Age Institute Press, Bloomington, pp. 181-198.
- 980 Kuman, K., Clarke, R.J., 2000. Stratigraphy, artefact industries and hominid associations for Sterkfontein,
981 Member 5. *Journal of Human Evolution* 38, 827-847.
- 982 Kurashina, H., 1978. An examination of prehistoric lithic technology in east-central Ethiopia. Unpublished
983 Ph.D. Dissertation, University of California, Berkeley.
- 984 Kyara, O.A., 1999. *Lithic Raw Materials and Their Implications on Assemblage Variation and Hominid*
985 *Behavior During Bed II, Olduvai Gorge, Tanzania*, University of Rutgers, New Brunswick, p. 876.
- 986 Leakey, L.S.B., 1951. *Olduvai Gorge, vol. 1*. Cambridge University Press, Cambridge.
- 987 Leakey, M.D., 1971. *Olduvai Gorge, vol. 3. Excavations in Beds I and II, 1960-1963*. Cambridge University
988 Press, Cambridge.
- 989 Leakey, MD., 1975. Cultural Patterns in the Olduvai Sequence. In: Butzer, K.W., Isaac, G.L. (Eds.). *After the*
990 *Australopithecines. Stratigraphy, Ecology, and Cultural Change in the Middle Pleistocene*. Mouton,
991 Chicago, pp. 477-493.
- 992 Leakey, M. D., 1976. The early stone industries of Olduvai Gorge, Tanzania. In: Clark, D., Isaac G.L. (Eds.), *Les*
993 *plus anciennes industries en Afrique*. Union Internationales des Sciences Préhistoriques et
994 *Protohistoriques*. IXe Congrès, UISPP, Nice, pp. 24-41.
- 995 Leakey, M. D. 1978: *Olduvai Gorge 1911–1975: a history of the investigations*. In Bishop, W. W. (ed.):
996 *Geological Background to Fossil Man: Recent Research in the Gregory Rift Valley, East Africa*. Scottish
997 Academic Press, Edinburgh, 151–155.

- 998 Lenoble, A., Bertran, P., 2004. Fabric of Palaeolithic levels: methods and implications for site formation
999 processes. *Journal of Archaeological Science* 31, 457-469. [Doi.org/10.1016/j.jas.2003.09.013](https://doi.org/10.1016/j.jas.2003.09.013)
- 1000 Ludwig, B.V., Harris, J.W.K., 1998. Towards a technological reassessment of East African Plio-Pleistocene
1001 lithic assemblages. In: Petraglia, M.D., Korisettar, R. (Eds.), *Early Human Behaviour in Global Context.*
1002 *Rise and Diversity of the Lower Paleolithic Record*. Routledge, London, pp. 84-107.
- 1003 McPherron, S.J.P., 2005. Artifact orientations and site formation processes from total station proveniences.
1004 *Journal of Archaeological Science* 32, 1003-1014. [Doi.org/10.1016/j.jas.2005.01.015](https://doi.org/10.1016/j.jas.2005.01.015)
- 1005 Pales, L., Lambert, C., 1971. *Atlas ostéologique pour servir à l'identification des mammifères du*
1006 *Quaternaire*. Editions du centre national de la recherche scientifique, Paris.
- 1007 Panera Gallego, J., Rubio-Jara, S., 1996. Propuesta de análisis tecnomorfológico para la industria lítica del
1008 Pleistoceno Medio. *Espacio, Tiempo y Forma. Serie I, Prehistoria y Arqueología* 9, 33–76.
- 1009 Pebesma, E. J., 2004. Multivariable geostatistics in S: the gstat package. *Computational Geosciences* 30,
1010 683–691.
- 1011 Petraglia, M. D., Potts, R., 1994. Water flow and the formation of Early Pleistocene artifact sites in Olduvai
1012 Gorge, Tanzania. *Journal of Anthropological Archaeology* 13 (3), 228–254. [https://doi.org/10.1006](https://doi.org/10.1006/jaar.1994.1014)
1013 [/jaar.1994.1014](https://doi.org/10.1006/jaar.1994.1014).
- 1014 Presnyakova, D., Braun, D. R., Conard, N. J., Feibel, C., Harris, J. W., Pop, C. M., Schlager, S., Archer, W.,
1015 2018. Site fragmentation, hominin mobility and LCT variability reflected in the early Acheulean record
1016 of the Okote Member, at Koobi Fora, Kenya. *Journal of Human Evolution* 125, 159-180.
- 1017 Quade, J., Levin, N., Semaw, S., Renne, P., Rogers, M. J., Simpson, S., 2004. Paleoenvironments of the
1018 earliest stone toolmakers, Gona, Ethiopia. *Geological Society of America Bulletin* 16, 1529–1544.
- 1019 Quade, J., Levin, N., Simpson, S., Butler, R., McIntosh, W., Semaw, S., Kleinsasser, L., Dupont-Nivet, G.,
1020 Renne, P., Dunbar, N., 2008. The Geology of Gona, Afar, Ethiopia. *Geological Society of America*
1021 *Bulletin, Special Papers* 446, 1–31.
- 1022 Roche, H., Brugal, J.-P., Delagnes, A., Feibel, C., Harmand, S., Kibunjia, M., Prat, S., Teier, P.J., 2003. Les sites
1023 archéologiques plio-pléistocènes de la formation de Nachukui, Ouest-Turkana, Kenya: bilan
1024 synthétique 1997–2001. *Comptes Rendus Palevol* 2, 663–673.
- 1025 Roger, S., Bivand, R. S., Pebesma, E. J., 2013. *Applied Spatial Data Analysis with R*. Springer, Heidelberg, 405
1026 pp.
- 1027 Romagnoli, F., Vaquero, M., 2016. Quantitative stone tools intra-site point and orientation patterns of a
1028 Middle Palaeolithic living floor: A GIS multi-scalar spatial and temporal approach. *Quatar* 63, 47-60.
1029 [Doi.org/10.7485/QU63_3](https://doi.org/10.7485/QU63_3)
- 1030 Rubio-Jara, S., Panera, J., Santonja, M., Pérez-González, A., Yravedra, J., Domínguez-Rodrigo, M., Bello, P.,
1031 Rojas, R., Mabulla, A., Baquedano, E., 2017. Site function and lithic technology in the Acheulean
1032 technocomplex: a case study from Thiongo Korongo (TK), Bed II, Olduvai Gorge, Tanzania. *Boreas*.
1033 <https://doi.org/10.1111/bor.12275>. ISSN 0300-9483.
- 1034 Sahnouni, M., 1991. Étude comparative des galets taillés polyédriques, subsphériques et sphériques des
1035 gisements d'Ain Hanech (Algérie Orientale) et d'Olduvai (Tanzanie). *L'Anthropologie* 97, 51-68.

- 1036 Sahnouni, M., Semaw, S., Rogers, M., 2013: The African Acheulean. An archaeological summary. In:
1037 Mitchell, P., Lane, P. (Eds.), *The Oxford Handbook of African Archaeology*, Oxford University Press,
1038 Oxford, pp. 307–323.
- 1039 Sánchez-Yustos, P., Díez-Martín, F., Domínguez-Rodrigo, M., Fraile, C., Duque, J., Uribelarrea, D., Mabulla,
1040 A., Baquedano, E., 2016. Techno-economic human behavior in a context of recurrent megafaunal
1041 exploitation at 1.3 Ma. Evidence from BK4b (Upper Bed II, Olduvai Gorge, Tanzania). *Journal of*
1042 *Archaeological Science: Reports* 9, 386-404.
- 1043 Sánchez-Yustos, P., Díez-Martín, F., Domínguez-Rodrigo, M., Tarriño Vinagre, A., 2012. Discriminación
1044 experimental de los rasgos técnicos en la talla bipolar y a mano alzada en lascas a través de los
1045 cuarzos de Naibor Soit (Garganta de Olduvai, Tanzania). *Munibe* 63, 5-26.
- 1046 Santonja, M., Panera, J., Rubio-Jara, S., Pérez-González, A., Uribelarrea, D., Domínguez-Rodrigo, M.,
1047 Mabulla, A.Z.P., Bunn, H.T., Baquedano, E. 2014. Technological strategies and the economy of raw
1048 materials in the TK (Thiongo Korongo) lower occupation, Bed II, Olduvai Gorge, Tanzania. *Quaternary*
1049 *International* 322-323, 181–208.
- 1050 Santonja, M., Rubio-Jara, S., Panera, J., Pérez-González, A., Rojas-Mendoza, R., Domínguez-Rodrigo, M.,
1051 Mabulla, A.Z.P., Baquedano, E., 2018. The Bifacial shaping in the TK Acheulean site (Bed II, Olduvai
1052 Gorge, Tanzania): New excavations 50 years after Mary Leakey. In: Galloti, R., Mussi, M. (Eds.), *The*
1053 *Emergence of the Acheulean in East Africa in East African and Beyond. Contributions in Honor of Jean*
1054 *Chavaillon. Vertebrate Paleobiology and Paleoanthropology Series. Springer*, pp. 153-181.
- 1055 Schick, K., 1986. Stone Age sites in the making: experiments in the formation and transformation of
1056 archaeological occurrences. *British Archaeological Reports*, Oxford.
- 1057 Semaw, S., Rogers, M. J., Cáceres, I., Stout, D., Leiss, A. C., 2018. The Early Acheulean~ 1.6–1.2 Ma from
1058 Gona, Ethiopia: Issues related to the Emergence of the Acheulean in Africa. In: Galloti, R., Mussi, M.
1059 (Eds.), *The Emergence of the Acheulean in East Africa in East African and Beyond. Contributions in*
1060 *Honor of Jean Chavaillon. Vertebrate Paleobiology and Paleoanthropology Series. Springer*, pp. 115-
1061 128.
- 1062 Shackley, M. L., 1974. Stream abrasion of flint implements. *Nature* 248 (5448), 501.
- 1063 Sharon, G., 2007. Acheulean large flake industries: Technology, chronology, and significance. *BAR (British*
1064 *Archaeological Reports) International Series* 1701. Oxford: Archaeopress.
- 1065 Sharon, G., 2010. Large flake Acheulean. *Quaternary International*, 223–224, 226–233.
- 1066 Shea, J. J., 1999. Artifact abrasion, fluvial processes, and “living floors” from the Early Paleolithic site
1067 of Ubeidiya (Jordan Valley, Israel). *Geoarchaeology* 14(2), 191-207.
- 1068 Silverman, B.W., 2018. *Density estimation for statistics and data analysis*. Routledge, London
- 1069 Stiles, D., 1977. Acheulian and developed Oldowan: the meaning of variability in the early Stone Age. *Mila*
1070 6, 1-35.
- 1071 Stiles, D., 1979. Early Acheulean and Developed Oldowan. *Current Anthropology* 20, 126–129.
- 1072 Stout, D., 2011. Stone toolmaking and the evolution of human culture and cognition. *Philosophical*
1073 *Transactions of the Royal Society B: Biological Sciences* 366(1567), 1050-1059.

- 1074 Texier, P.-J., 1995. The Oldowan assemblage from NY18 site at Nyabusosi (Toro-Uganda). *C.R.Acad.Sci.Paris*
1075 320, série Ila, 647-653.
- 1076 Texier, P.-J., 2005. L'Oldowayen dans le Grand Rift occidental: le site NY18 à Nyabusosi (Ouganda). In:
1077 Sahnouni, M. (Ed.), *Le Paléolithique en Afrique, l'Histoire la Plus Longue*, Paris. Artcom, pp. 83–98.
- 1078 Texier, P. J., 2018. Technological Assets for the Emergence of the Acheulean? Reflections on the Kokiselei 4
1079 Lithic Assemblage and Its Place in the Archaeological Context of West Turkana, Kenya. In: Galloti, R.,
1080 Mussi, M. (Eds.), *The Emergence of the Acheulean in East Africa in East African and Beyond. Contributions in Honor of Jean Chavaillon. Vertebrate Paleobiology and Paleoanthropology Series.*
1081 Springer, pp. 33-52.
- 1083 Thompson, C.E., Ball, S., Thompson, T.J.U., Gowland, R., 2011. The abrasion of modern and archaeological
1084 bones by mobile sediments: the importance of transport modes. *Journal of Archaeological Science* 38,
1085 784-793.
- 1086 Tixier, J., 1956. Le hachereau dans l'Acheuléen Nord-Africain. Notes typologiques. Congrès Préhistorique de
1087 France, XVème session (Poitiers), pp. 914-923.
- 1088 de la Torre, I., 2004. Estrategias tecnológicas en el Pleistoceno inferior de África oriental (Olduvai y Peninj,
1089 norte de Tanzania). Tesis doctoral. Universidad Complutense, Madrid.
- 1090 de la Torre, I., 2011. The early stone age lithic assemblages of Gadeb (Ethiopia) and the developed
1091 Oldowan/early Acheulean in East Africa. *Journal of Human Evolution* 60(6), 768-812.
- 1092 de la Torre, I., Albert, R. M., Macphail, R., McHenry, L. J., Pante, M. C., Rodríguez-Cintas, Á., Stanistreet, I.G.,
1093 Stollhofen, H., 2018. The contexts and early Acheulean archaeology of the EF-HR paleo-landscape
1094 (Olduvai Gorge, Tanzania). *Journal of Human Evolution*, 120, 274-297.
- 1095 de la Torre, I., Mora, R., 2005. Technological Strategies in the Lower Pleistocene at Olduvai Beds I and II.
1096 University of Liège Press, ERAUL 112. p. 247.
- 1097 de la Torre, I., Mora, R., 2013. The Transition to the Acheulean in East Africa: An Assessment of Paradigms
1098 and Evidence from Olduvai Gorge (Tanzania). *Journal of Archaeological Method and Theory* 21, 781.
1099 DOI 10.1007/s10816-013-9176-5.
- 1100 Turq, A., 2000. Paléolithique inférieur et moyen entre Dordogne et Lot. *Paléo (Supplément 2)*, p. 454.
- 1101 Uribelarrea, D., Martín-Perea, D., Díez-Martín, F., Sánchez-Yustos, P., Domínguez-Rodrigo, M., Baquedano,
1102 E., Mabulla, A., 2017. A reconstruction of the paleolandscape during the earliest Acheulian of FLK
1103 West: The co-existence of Oldowan and Acheulian industries during lowermost Bed II (Olduvai Gorge,
1104 Tanzania). *Palaeogeography, Palaeoclimatology, Palaeoecology* 488, 50-58.
- 1105 Villa, P., Courtin, J., 1983. The interpretation of stratified sites: a view from underground. *Journal of*
1106 *Archaeological Science*, 10 (3), 267–281.
- 1107 Villa, P., Mahieu, E., 1991. Breakage patterns of human long bones. *Journal of Human Evolution* 21, 27-48.
- 1108 Whallon, R., 1973. Spatial analysis of occupation floors I: application of dimensional analysis of variance.
1109 *American Antiquity* 38, 266–278.
- 1110 Whallon, R., 1974. Spatial analysis of occupation floors II: the application of nearest neighbor analysis.
1111 *American Antiquity* 39, 16–34.

- 1112 Willoughby, P.R., 1987. Spheroids and Battered Stones in the African Early Stone Age. Oxford. In: British
1113 Archaeological Research International Series 321.
- 1114 Yellen, J.E., 1977. Archaeological approaches to the present: models for reconstructing the past. Serie:
1115 Studies in Archaeology. New York. Academic Press.
- 1116 Yravedra, J., Domínguez-Rodrigo, M., 2009. The shaft-based methodological approach to the quantification
1117 of long limb bones and its relevance to understanding hominin subsistence in the Pleistocene:
1118 application to four Paleolithic sites. *Journal of Quaternary Science* 24, 85-96.
- 1119 Yravedra, J., Domínguez-Rodrigo, M., Santonja, M., Rubio-Jara, S., Panera, J., Pérez-González, A.,
1120 Uribelarrea, D., Egeland, C., Mabulla, A.Z.P., Baquedano, E. 2016. The larger mammal palimpsest
1121 from TK (Thiongo Korongo), Bed II, Olduvai Gorge, Tanzania. *Quaternary International* 417, 3-15.

Journal Pre-proof

Chaîne opératoire phases at TKSF	Unworked items			Used, retouched, or shaped items			Total		
	a	b	c	a	b	c	a	b	c
0. Procurement phase		24	7	4	27	3	4	51	10
1.1. First reduction phase	29	1		3	1		32	2	
1.2. Full reduction phase	257	16		11	1		268	17	
1.3. Full reduction phase (backed products)	11			10	1		21	1	
1.4. Cores	61	7		21	2		82	9	
<i>Subtotal of production phase</i>	358	24		45	5		403	29	
2. Façonnage and retouched items on natural blank									
2.1. Handaxes, preforms and fragments				30	7		30	7	
2.2. Trihedral picks				8			8		
2.3. Cleavers				4			4		
2.4. Large scrapers & retouched slabs				4			4		
<i>Subtotal of façonnage phase</i>				46	7		46	7	
3. Shatter	605	5	1				605	5	1
Total	963	53	8	95	39	3	1058	92	11
Total: 1161 pieces									

Table 1. *Chaîne opératoire* phases identified at TKSF. a. Naibor quartzite, b. Volcanic rocks, c. and other rocks; 0. Procurement phase includes cobbles, hammerstone detachments (basalt fragments with no percussion platform nor bulb produced by a hammerstone), cobbles with pits, and slabs with percussion marks; 1.1. First reduction phase produces highly cortical flakes (>90% cortex), cortical flakes (50-90% cortex), and cortical flake fragments when the flakes have small fractures which do not prevent determination of the cortex percentage. 1.2. Full reduction phase produces ordinary products: flakes with cortex removed (<10% cortex), partly cortical flakes (10-50% cortex), flake fragments with cortex removed and Janus flakes. 1.3. Full reduction phase produces backed items: flakes and flake fragments with debitage back or cortical back. 1.4. Cores (on slab, cobble, flake, or undetermined blank); 2. Façonnage phase; 3. Shatter or undifferentiated products. They are by-products of the *chaîne opératoire* but are not specific to any particular phase, and can be originated by both bipolar and freehand knapping. Shatter includes debris (produced during knapping and does not present a defined butt or bulb), chunks (core waste that display removal traces but cannot be assigned to any category of cores) and angular fragments (usually polyhedral, of any size, and produced during the knapping of NQ slabs, as it generates a large number of uncontrolled fractures).

	NISP	MNI
<i>Elephas sp</i>	4	1
<i>Hippopotamus sp</i>	19	1
<i>Sivatherium</i>	12	1
<i>Syncerus sp.</i>	3	1
<i>Alcelaphini 3b</i>	3	1
<i>Equus oldowayensis</i>	6	1
<i>Metridiochoerus sp.</i>	3	1
<i>Suidae size 3</i>	1	
<i>Suidae size 2</i>	2	
Indet size 1	5	
Indet size 2	13	
Indet size 3	14	
Indet size 3a	7	
Indet size 3b	17	
Indet size 4	38	
Indet size 5	50	
Indet size 6	1	
Indet	140	
Total	338	7

Table 2. NISP and MNI of the animals identified taxonomically classified by size and weight in TKSF.

Animal Size:	1		2		3		3a		3b		4		5		6	
	NISP	%NISP	NISP	%NISP	NISP	%NISP	NISP	%NISP	NISP	%NISP	NISP	%NISP	NISP	%NISP	NISP	%NISP
Skull	1	25	-	-	-	-	-	-	-	-	-	-	-	-	-	-
Teeth	-	-	1	7.14	2	13.33	3	33.33	8	28.57	3	7.5	8	9.88	-	-
Mandible	-	-	-	-	1	6.67	-	-	1	3.57	-	-	-	-	-	-
Rib	1	25	4	28.57	1	6.67	-	-	4	14.29	10	25	21	25.93	1	20
Vertebrae	-	-	-	-	1	6.67	-	-	1	3.57	3	7.5	12	14.81	-	-
Scapulae	-	-	-	-	-	-	-	-	1	3.57	1	2.5	3	3.7	-	-
Pelvis	-	-	-	-	-	-	-	-	2	7.14	1	2.5	6	7.41	-	-
Humerus	-	-	-	-	-	-	-	-	-	-	-	-	4	4.94	-	-
Radius	-	-	1	7.14	-	-	-	-	-	-	-	-	-	-	-	-
Ulna	-	-	-	-	-	-	-	-	1	3.57	-	-	-	-	-	-
Femur	-	-	-	-	-	-	1	11.11	1	3.57	-	-	3	3.7	-	-
Tibiae	-	-	-	-	2	13.33	-	-	1	3.57	1	2.5	2	2.47	-	-
Metacarpal	-	-	-	-	-	-	-	-	1	3.57	-	-	1	1.23	-	-
Metatarsal	-	-	2	14.29	-	-	1	11.11	-	-	1	2.5	3	3.7	-	-
Metapodial	-	-	1	7.14	-	-	1	11.11	3	10.71	1	2.5	2	2.47	-	-
Carpal	-	-	1	7.14	1	6.67	1	11.11	1	3.57	-	-	4	4.94	2	40
Tarsal	-	-	-	-	-	-	1	11.11	1	3.57	-	-	4	4.94	-	-
Phalange	1	-	1	7.14	-	-	-	-	-	-	1	2.5	1	1.23	-	-
Indet.	1	-	3	21.43	7	46.67	1	11.11	2	7.14	18	45	7	8.64	2	40
Total	4		14		15		9		28		40		81		5	

Table 3. TKSF Skeletal part profiles according NISP and %NISP.

Journal Pre-proof

	<i>Sivatherium sp</i>		<i>Hippopotamus sp</i>		<i>Syncerus sp.</i>		Indet size 4		Indet size 5	
	NISP	%NISP	NISP	%NISP	NISP	%NISP	NISP	%NISP	NISP	%NISP
Teeth	-	-	6	31.58	2	66.67	2	5.41	2	4
Vertebrae	4	33.33	2	10.53	-	-	2	5.41	7	14
Ribs	-	-	-	-	-	-	10	27.03	21	42
Scapulae	2	16.67	-	-	1	33.33	-	-	1	2
Coxal	1	8.33	1	5.26	-	-	1	2.7	3	6
Femur	1	8.33	-	-	-	-	-	-	2	4
Humerus	1	8.33	-	-	-	-	-	-	3	6
Tibia	2	16.67	-	-	-	-	1	2.7	-	-
Carpal / Tarsals	1	8.33	4	21.05	-	-	-	-	3	6
Metapodial	-	-	5	26.32	-	-	2	5.41	1	2
Phalange	-	-	1	5.26	-	-	-	-	-	-
Indeterminate	-	-	-	-	-	-	19	51.35	7	14

Table 4. TKSF NISP values of large animals of size groups 4 and 5.

Journal Pre-proof

	Fracture		Green fracture Planes		Circunference Degree		
	Green	Dry	Oblique	Longitudinal	I	C	O
Shaft	7 (30.43%)	16 (69.57%)	5 (71,4%)	2(28,6%)	8 (34.78%)	4 (17.39%)	11 (47.83%)

Table 5. Fracture types according to Villa and Mahieu (1991) regarding dry and green fractures, fracture planes for green fractures, and circumference degree of the diaphysis according to Bunn (1982), where I: <50%, C: >50% and O: complete circumference.

Journal Pre-proof

	NISP	Cut Marks	Percussion marks	Tooth Marks	Polishing and Abrasion	Carbonate- concretion	Trampling	Biochemical	Weathering	Poor preservation
NISP	326	3			265	235	47	19	29	231
%					81.3	72	14.4	5.8	8.6	70.86

Table 6. TKSf. Alterations recorded at TKSf.

Journal Pre-proof

Rounding	QN	VR	Other	Total
Fresh	989	86	10	1086
Light	53	3		55
Intense	11	2		13
Indeterminate	4	2	1	7
Total	1057	93	11	1161

Table 7. Rounding of the lithic industry: NQ, Naibor Quartzite; VR, Volcanic Rocks.

Journal Pre-proof

	Assemblage	n	Mean Vector (μ)	Length of Mean Vector (r)	Concentration	Circular Variance	Circular Standard Deviation	Rayleigh Test (Z)	Rayleigh Test (p)	Kuiper's Test (Uniform. V)	Kuiper's Test (p)
M B R	Industry	183	47.793°	0.09	0.181	0.455	62.842°	1.488	0.226	1.408	> 0.15
	Fauna	115	25.012°	0.132	0.266	0.434	57.679°	1.996	0.136	1.682	0.10 > p > 0.05
P M A	Industry	183	126.53°	0.118	0.237	0.441	59.273°	2.531	0.08	1.438	> 0.15
	Fauna	115	154.667°	0.145	0.292	0.428	56.347°	2.402	0.091	1.485	> 0.15

Table 8. The results of the main orientation analysis and of the Rayleigh and Kuiper's tests on the uniformity of all assemblages of TKSf.

Assemblage	n	Woodcock's index		Eigenvectors and Eigenvalues						Vollmer's index			Benn's index			
		K	C	V1	V2	V3	S1	S2	S3	Cluster	Girdle	Uniform	IS	EL	F	CGI
Industry MBG	183	0.66	1.04	268/51/31.157	13/12/59.989	112/37/90.854	0.317	0.275	0.215	0.169	0.304	0.527	0.677	0.134	0.781	0.556
Industry PMA	183	0.54	1.03	270/50/31.768	165/12/62.159	65/37/89.074	0.276	0.324	0.211	0.147	0.332	0.521	0.765	-0.176	0.650	0.443
Fauna MBG	115	0.16	1.95	275/67/8.3783	44/15/44.772	139/17/58.849	0.374	0.365	0.188	0.126	0.650	0.224	0.502	0.025	0.515	0.194
Fauna PMA	115	0.16	1.97	259/67/8.2736	136/13/44.722	42/19/59.005	0.370	0.363	0.188	0.128	0.651	0.222	0.509	0.019	0.519	0.197

Table 9. Fabric index of the TKSf archaeological remains.

Assemblage	Density			Nearest Neighbor index				Getis-Ord General G index			
	n	m ²	density / m ²	R	Z	p	Result	G	Z	p	Result
Total	1341	48.2	27.82	0.87	-8.65	0.000	Cluster	0.00	5.67	0.000	High-Cluster
Industry	1051	48.2	21.80	0.89	-5.80	0.000	Cluster	0.00	4.86	0.000	High-Cluster
Fauna	290	48.2	6.02	0.80	-5.51	0.000	Cluster	0.00	-5.21	0.000	Low-cluster
Flakes	328	48.2	6.80	0.91	-2.84	0.004	Cluster	0.00	4.49	0.00	High-Cluster
Shatter	520	48.2	10.79	0.84	-6.67	0.000	Cluster	0.00	4.90	0.000	High-Cluster
Cores	31	48.2	0.64	0.93	-1.14	0.251	Random	0.00	2.50	0.012	High-Cluster
LCT	48	48.2	1.00	0.93	-0.92	0.353	Random	0.00	1.04	0.295	Random
Cobble	52	48.2	1.08	1.13	1.92	0.053	Dispersed	0.16	-0.52	0.602	Random
Percussion materials	12	48.2	0.25	1.2	1.38	0.16	Random	0.00	1.04	0.298	Random

Table 10. Density and clustering values of the TKSF archaeological remains.

Captions

Fig. 1. A. Location of Thiongo Korongo (TK) at Olduvai Gorge (modified after Hay 1976); Location of TK in a lateral gully; Positions of the trenches excavated by M. Leakey (1963) and the sectors excavated by TOPPP (2010–2015), showing the areas occupied by the TKLF and the TKSf. B. Stratigraphical section showing the horizons excavated at TKSf.

Fig. 2. A, Lithic industry and faunal remains distribution; B, lithic industry distribution; C, faunal remains distribution; D distribution map of faunal remains with cut marks, percussions marks, and green fractures.

Fig. 3. Cut marks at TKSf. TK'2014, n° 8263: Animal size 5 rib; TK'2015, n° 8599: Size 3b metapodial.

Fig. 4. TKSf: Rose diagrams of the studied assemblages

Fig. 5. TKSf: Woodcock's diagram (upper) and Vollmer's diagram (below) (adapted from Lenoble, et al., 2008).

Fig. 6. TKSf: Stereographic projection of the main studied assemblages.

Fig. 7. TKSf. Kernel density maps: A) all assemblage; B) lithic industry; C) faunal remains.

Fig. 8. TKSf. Kernel density maps by lithic industry techno-typological categories: A) Percussion elements; B) cobbles; C) shatter; D) cores; E) flakes; F) LCTs.

Fig. 9. TKSf. K-means groups maps: A) all assemblage; B) lithic industry; C) faunal remains.

Fig. 10. TKSf. Cluster outlie maps: A) all assemblage; B) lithic industry; C) faunal remains.

Fig. 11. TKSf. Optimized hotspot: A) all assemblage; B) lithic industry; C) faunal remains.

Figure 12. Besag's inhomogeneous L-function applied to simulate a random inhomogeneous Poisson process (red dotted line), whose 95% confidence interval is shown as a gray global envelope. The TK bone and lithic data fall within the margins of the confidence envelope, showing that they are two inhomogeneous Poisson processes.

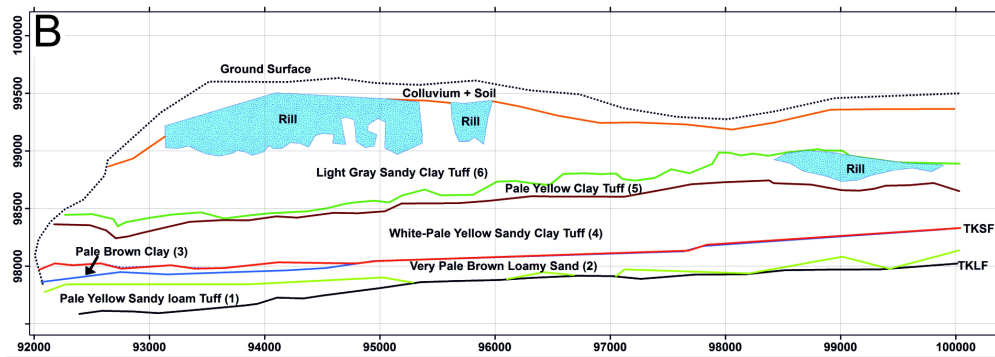
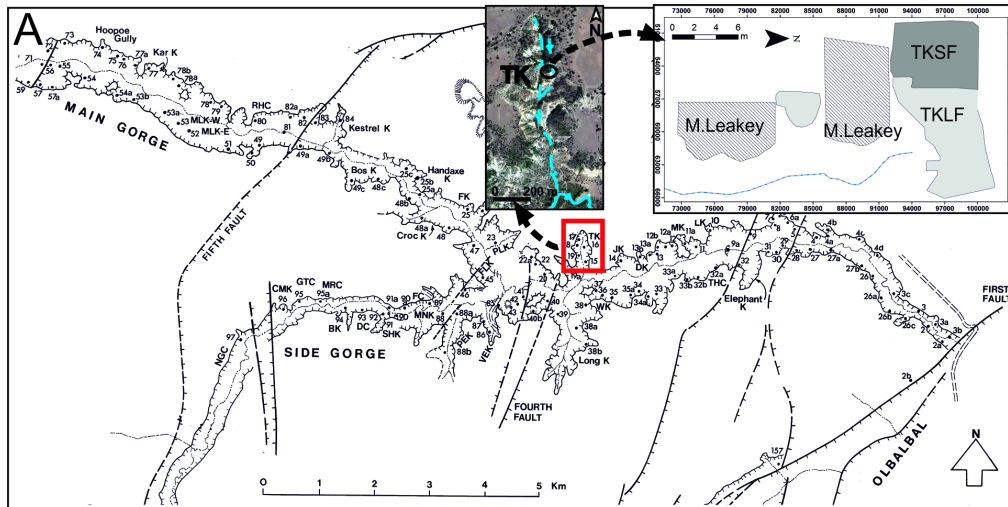
Figure 13. Besag's L-function test applied with a homogeneous (A-B) and an inhomogeneous (C-D) Poisson process for lithics (A-D) and bones (B-D). A confidence global envelope is displayed together with the theoretical Poisson process (red dotted line).

Figure 14. Kernel maps showing the distribution of lithics (A-C) and bones (B-D). Maps A and B were obtained using likelihood cross-validation. Maps C and D were obtained using adaptive intensity, based on Dirichlet-Voronoi estimation of density.

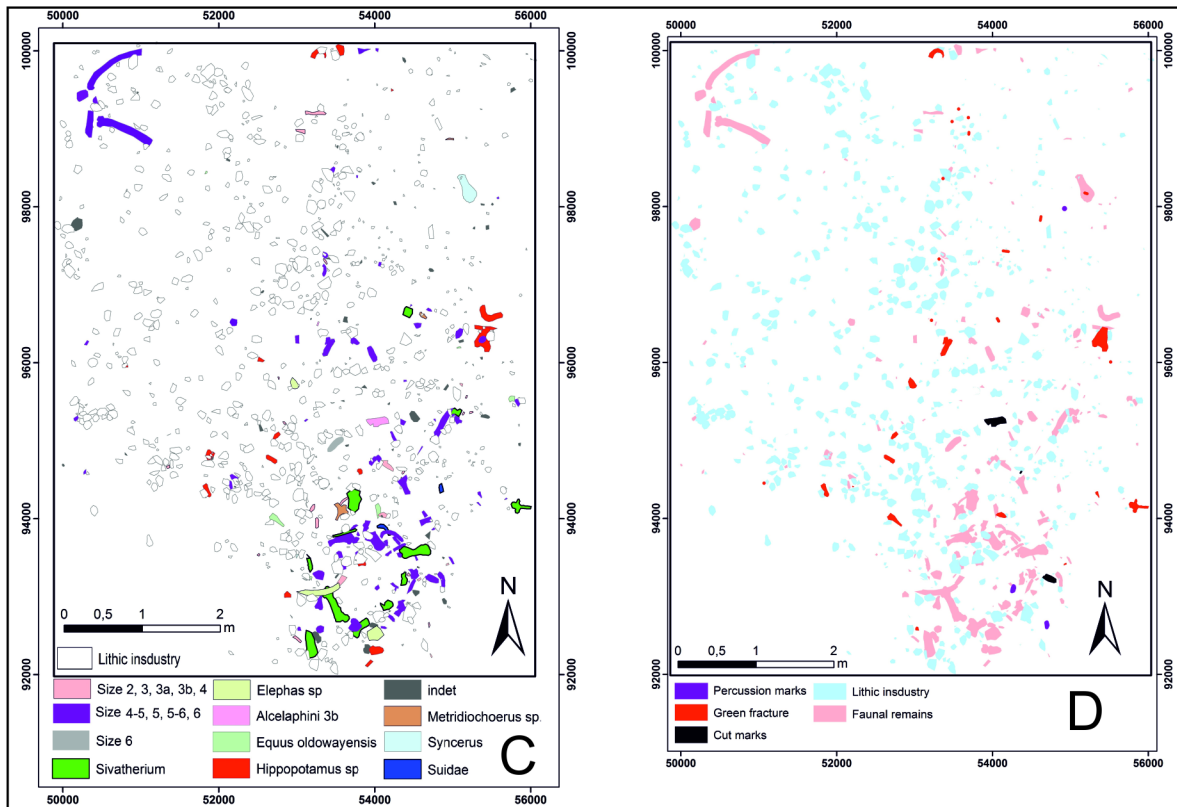
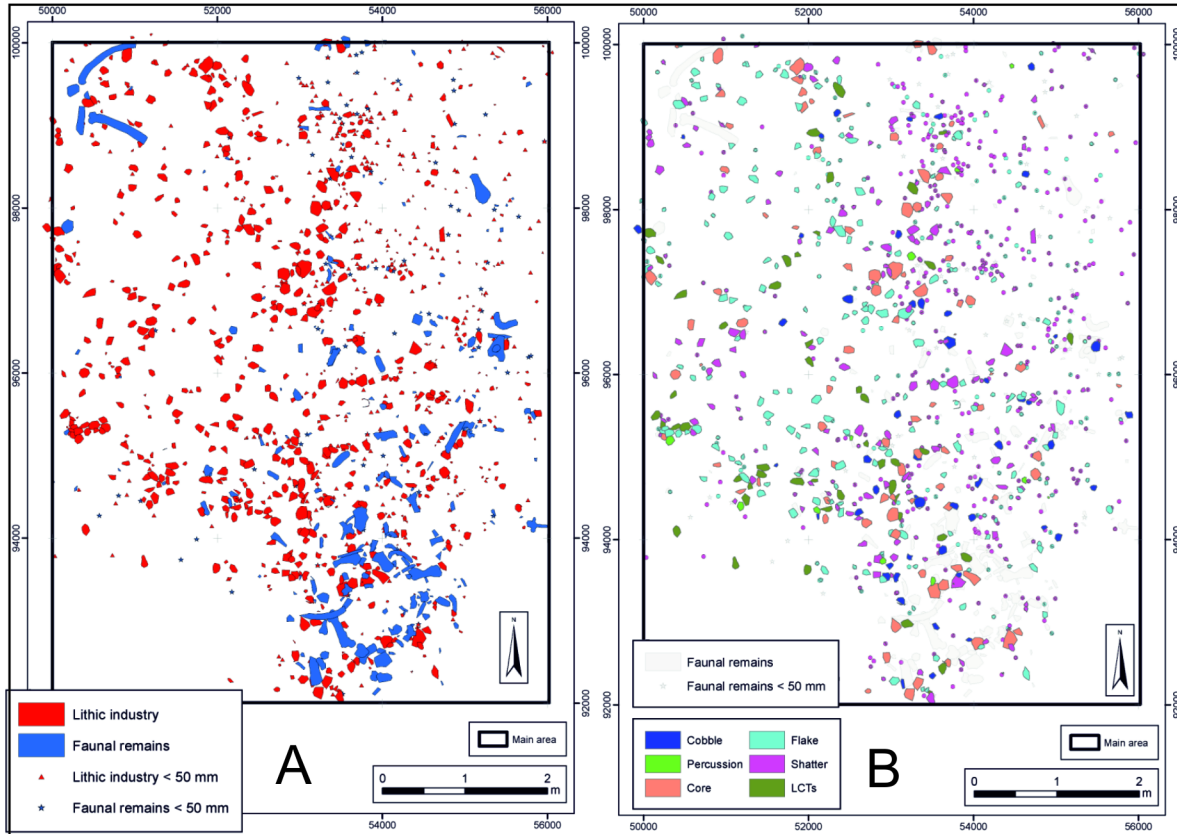
Figure 15. Random labelling using the J function. The TK bone-lithic point process shows random distribution within the confidence envelope indicating no strong co-dependence of fauna with lithics.

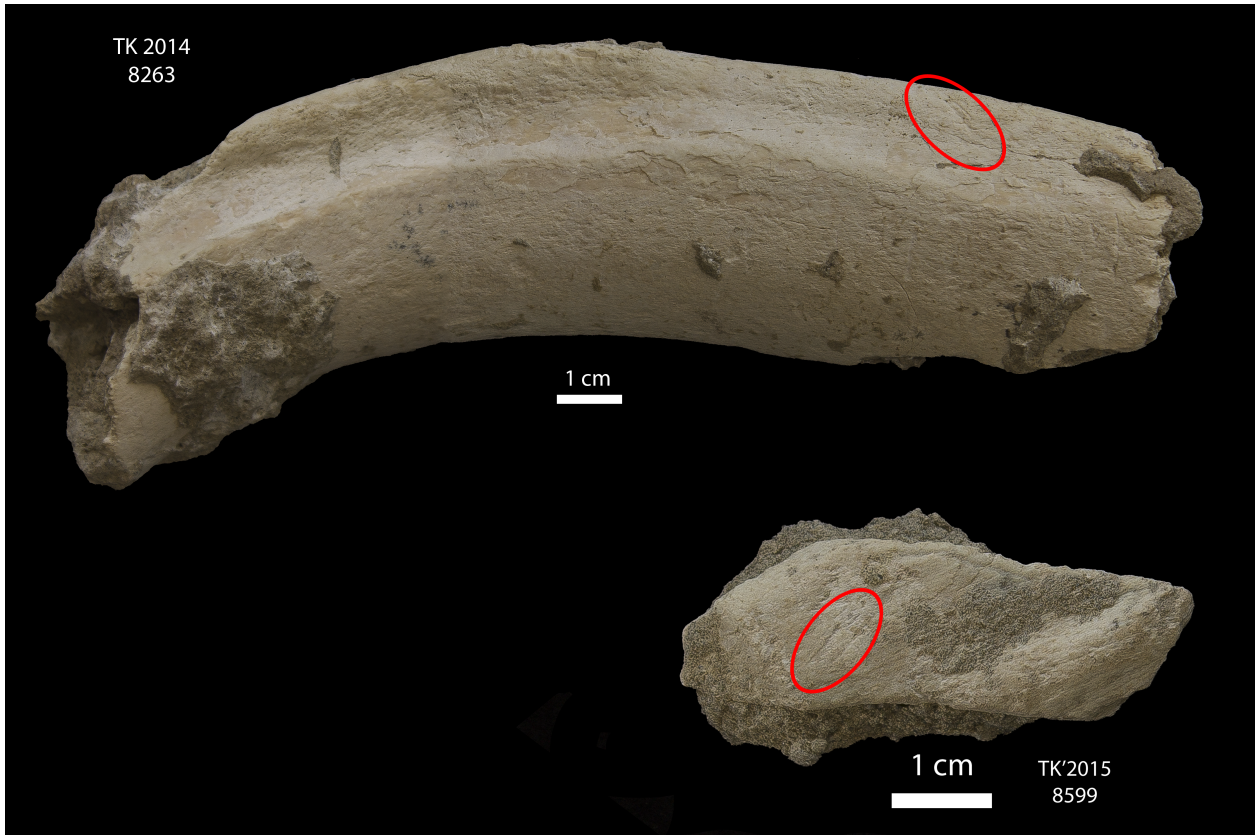
Figure 16. Cross-type analysis, using the inhomogeneous Besag's L-function. Fauna (f) and lithics (l) show local minor clustering (diagonal) and their interaction (off-diagonal) shows spatial clustering co-dependence.

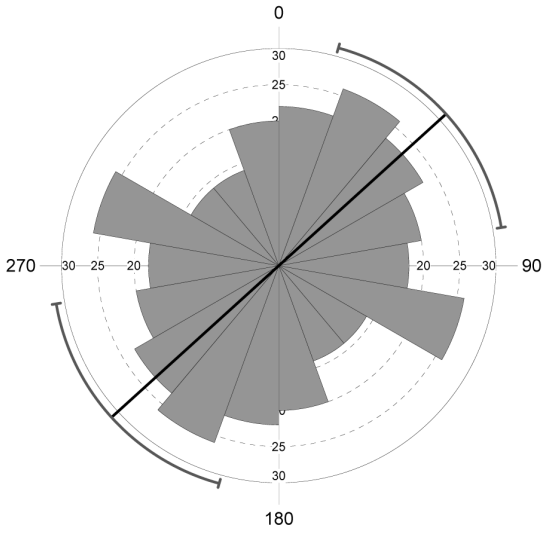
Journal Pre-proof



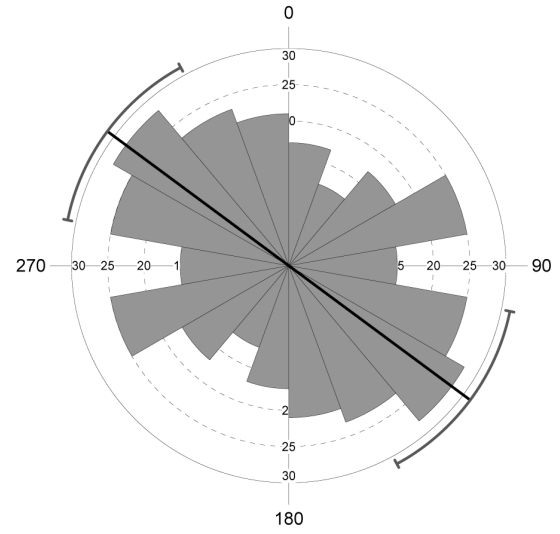
Journal



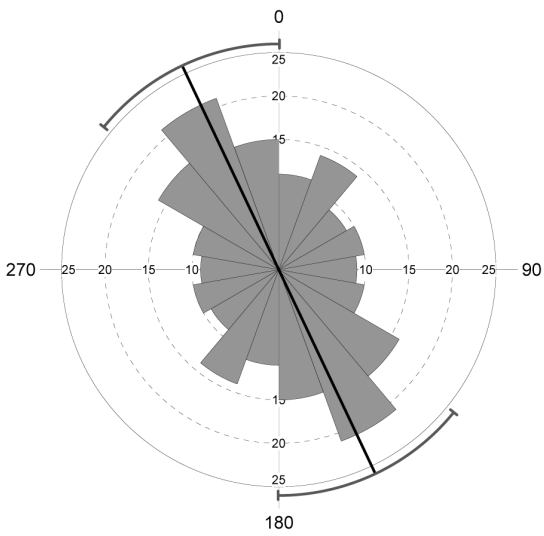




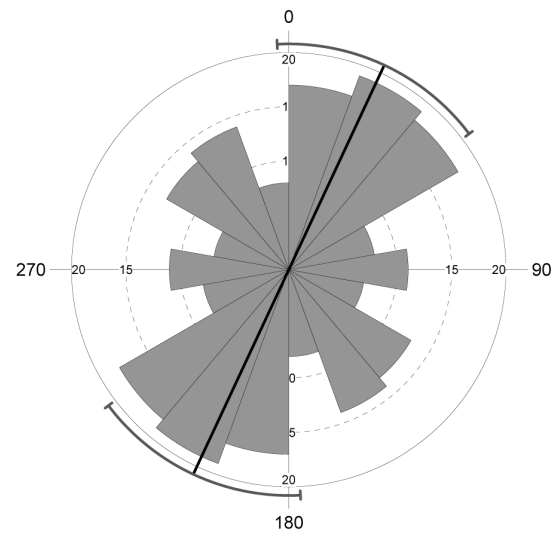
Lithic industry MBR



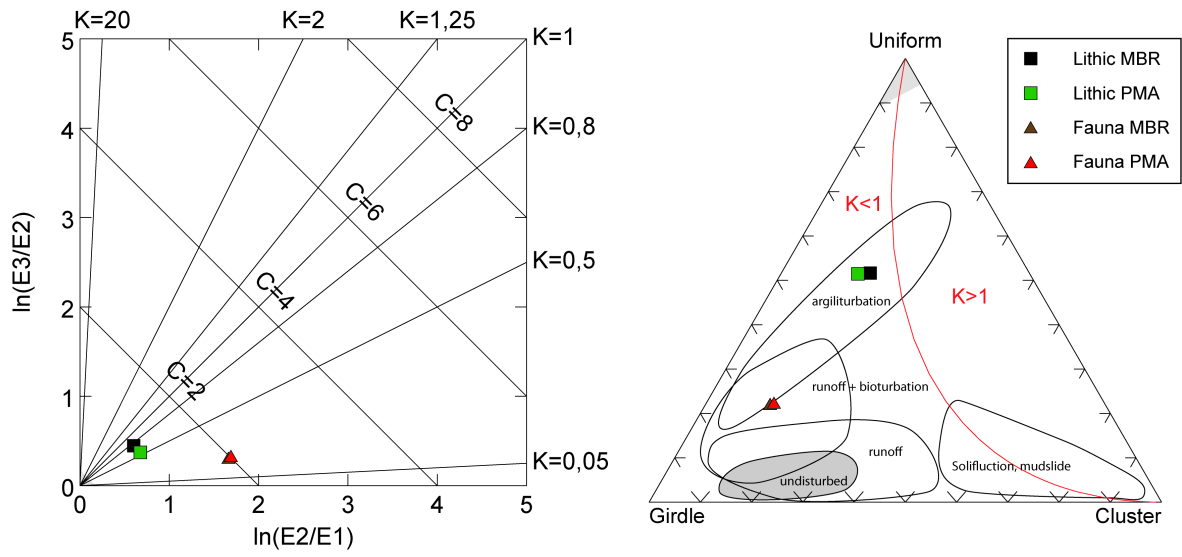
Lithic industry PMA

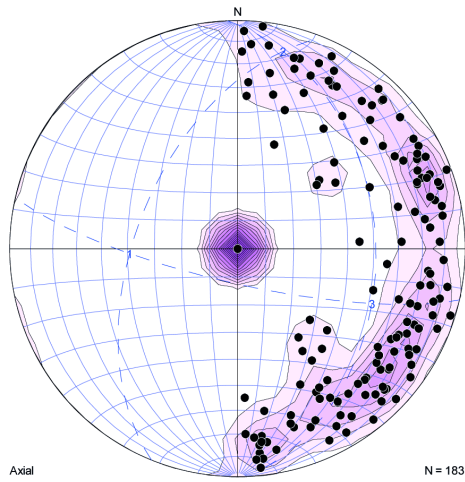


Faunal remains MBR

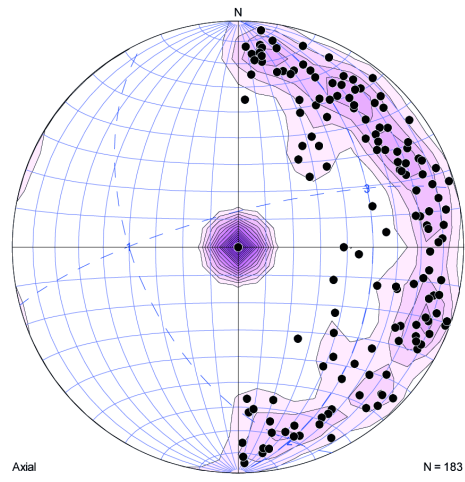


Faunal remains PMA

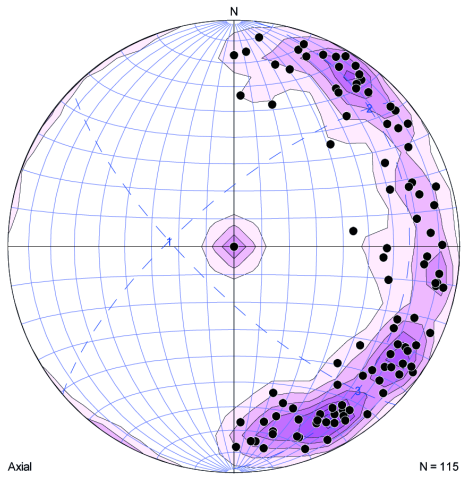




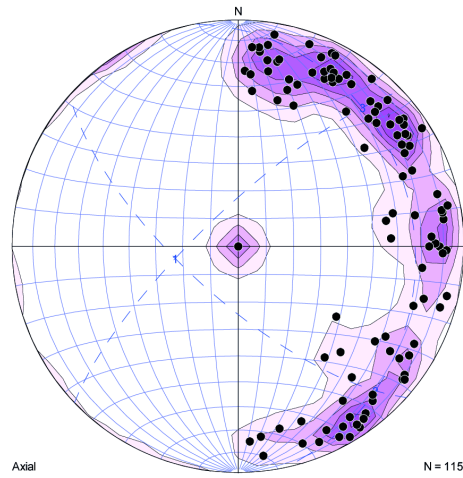
Lithic industry MBR



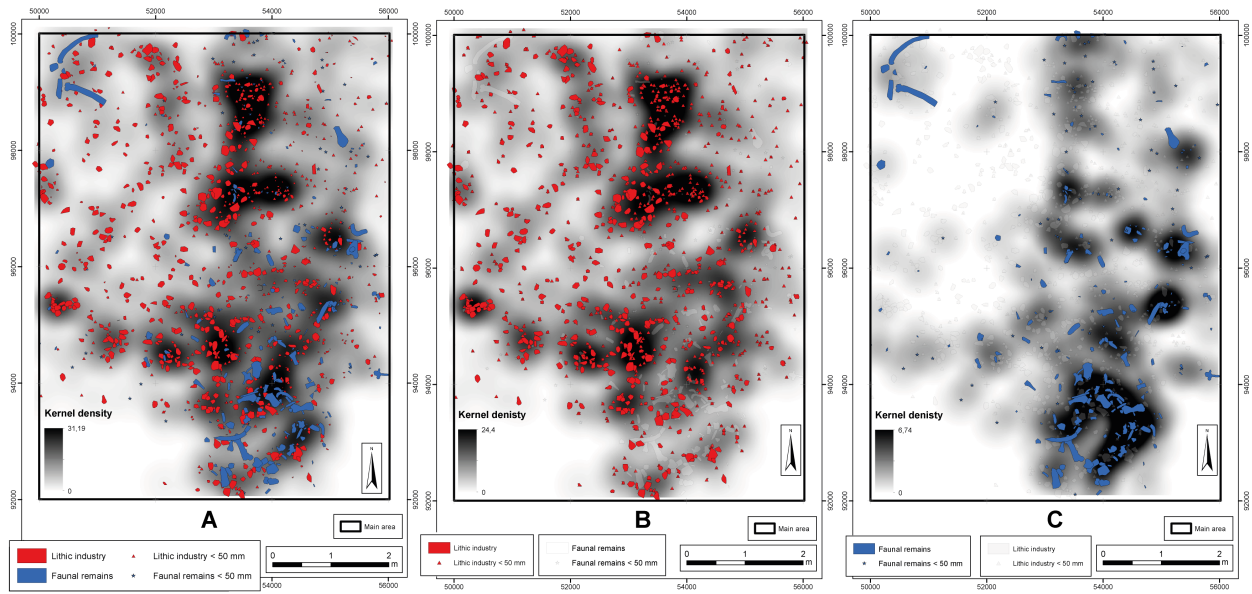
Lithic industry PMA

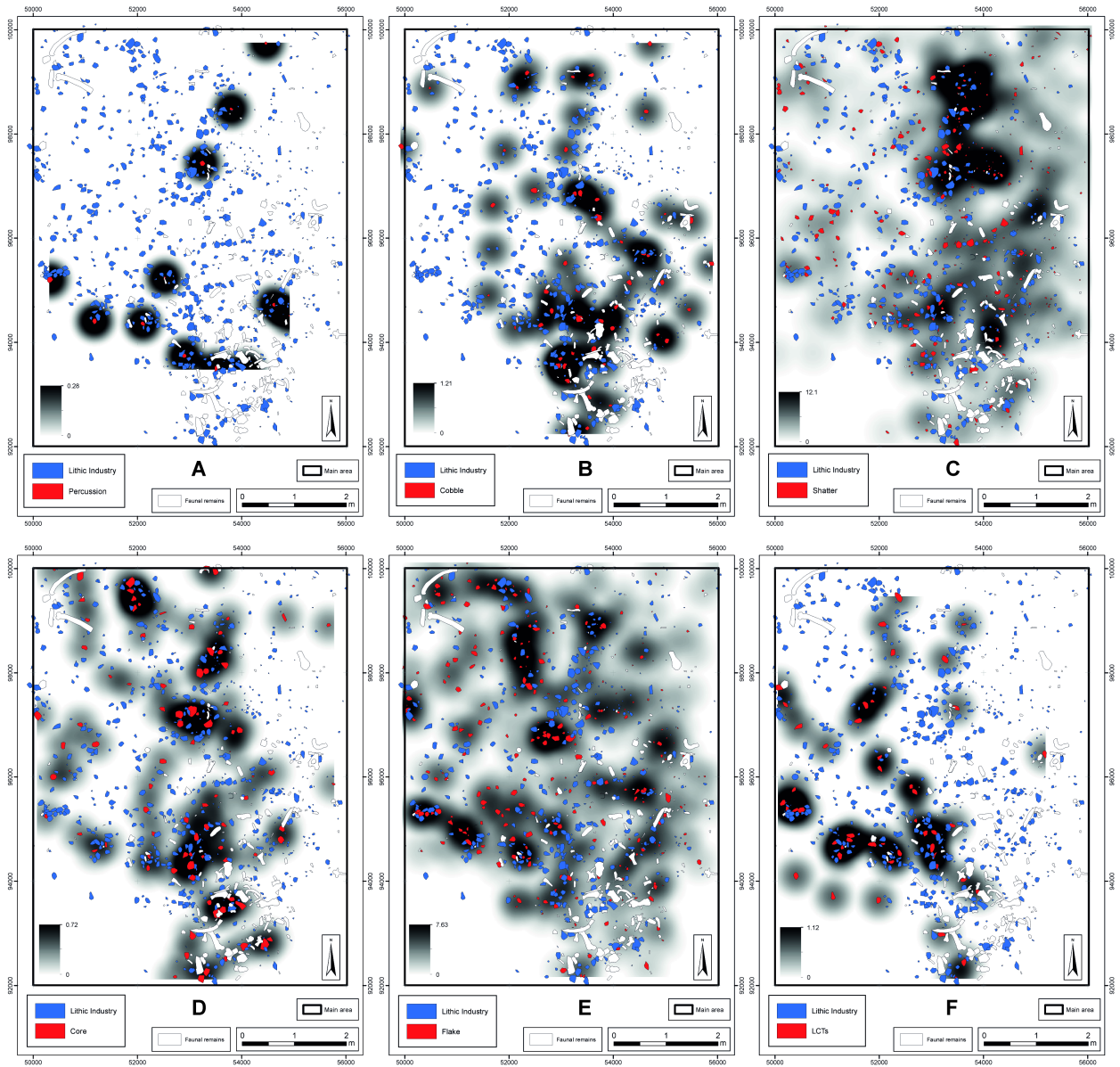


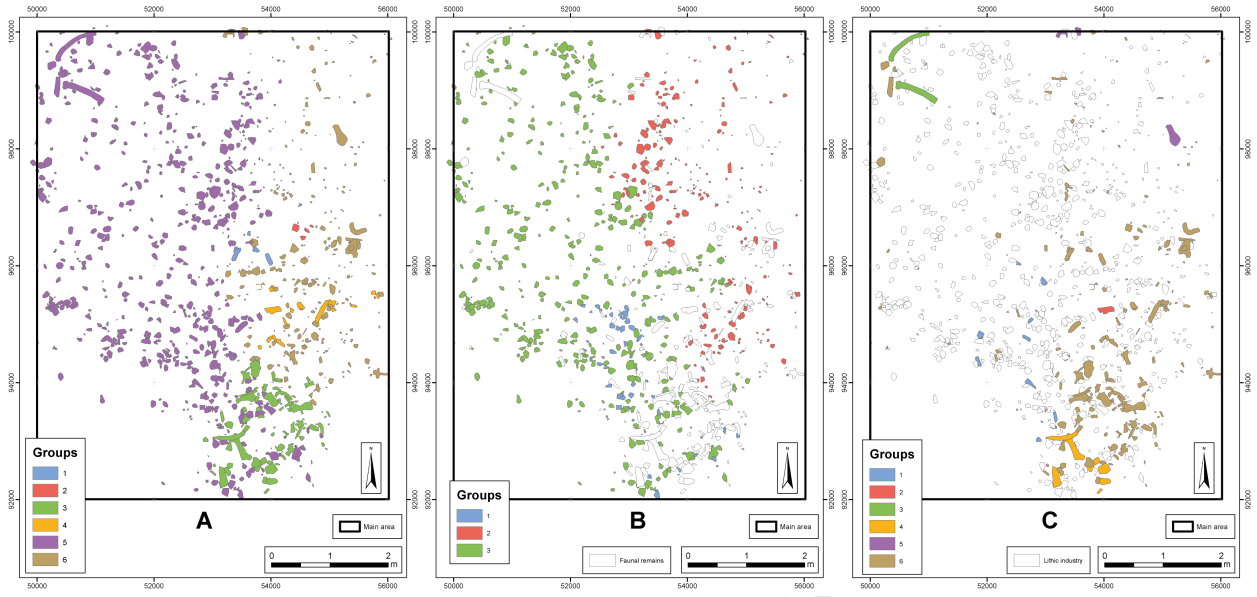
Faunal remains MBR

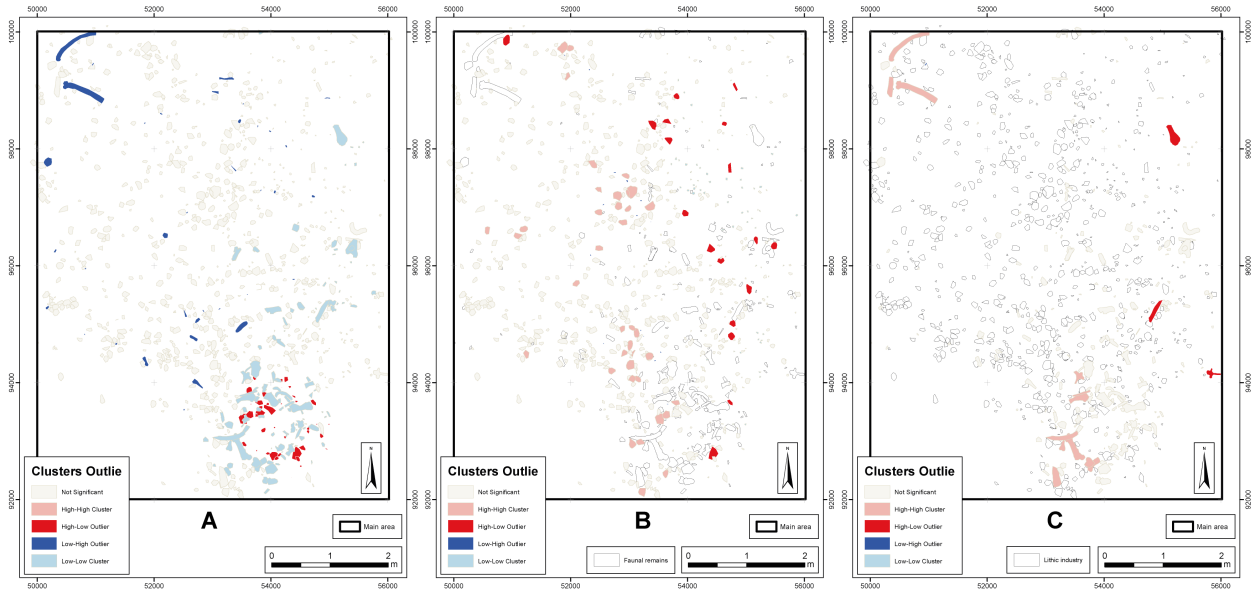


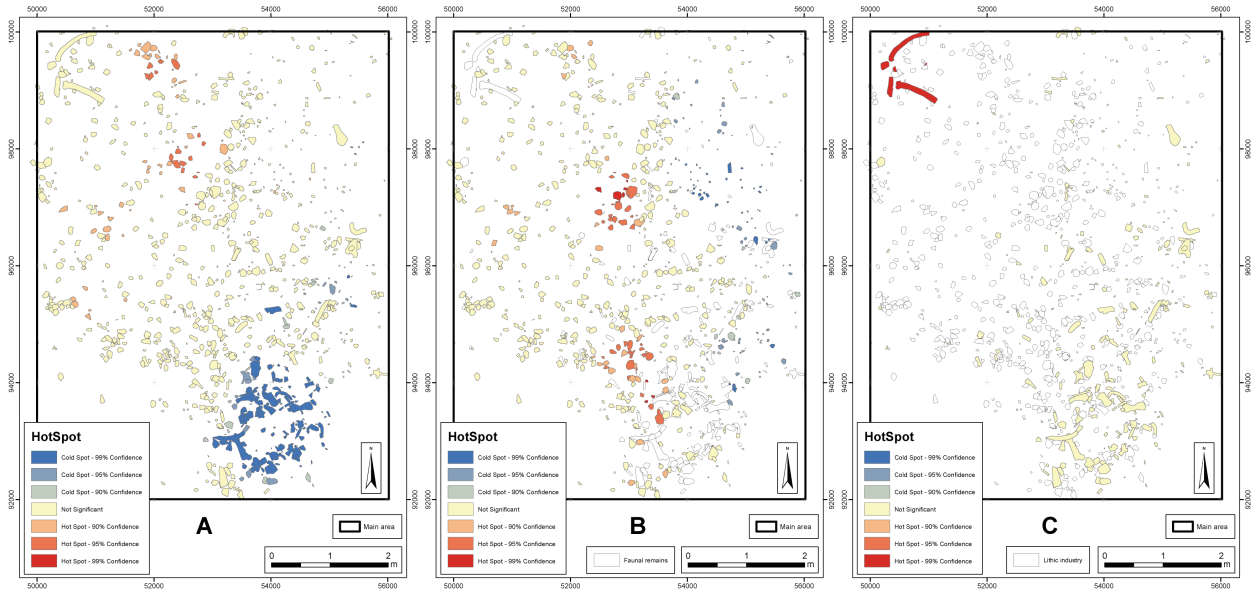
Faunal remains PMA

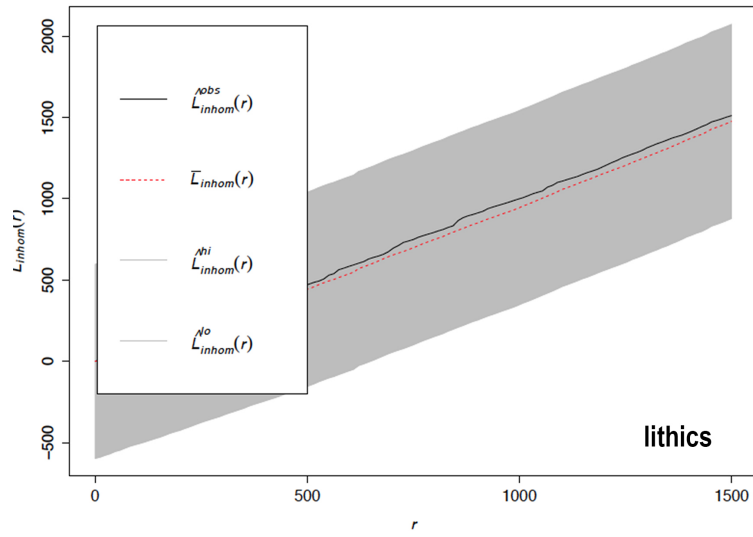
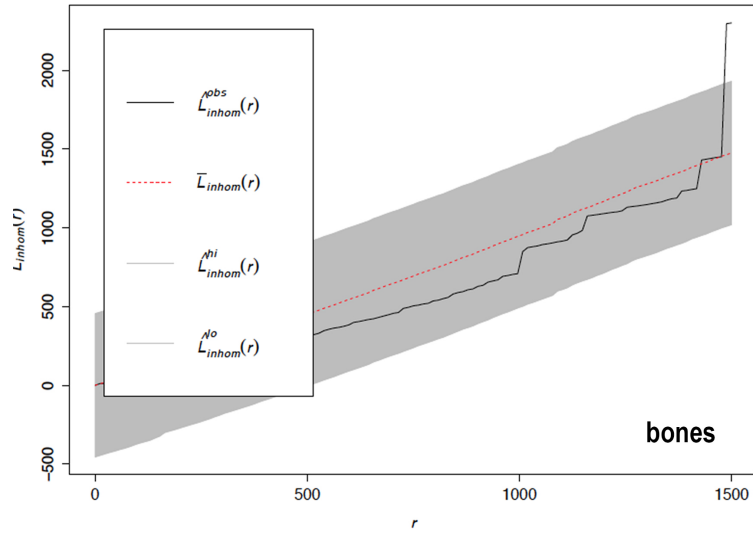




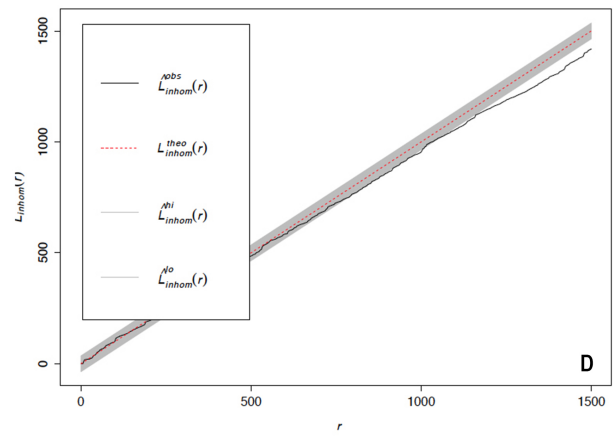
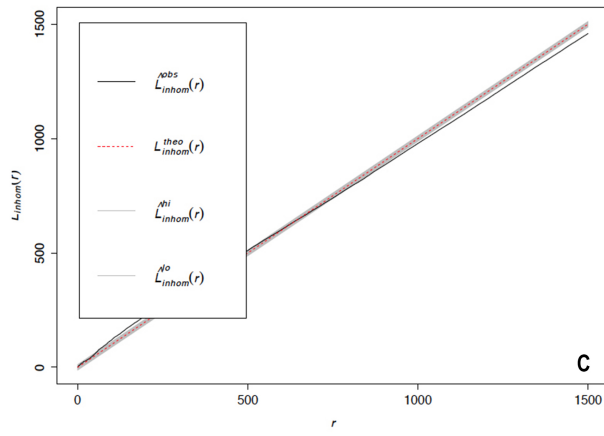
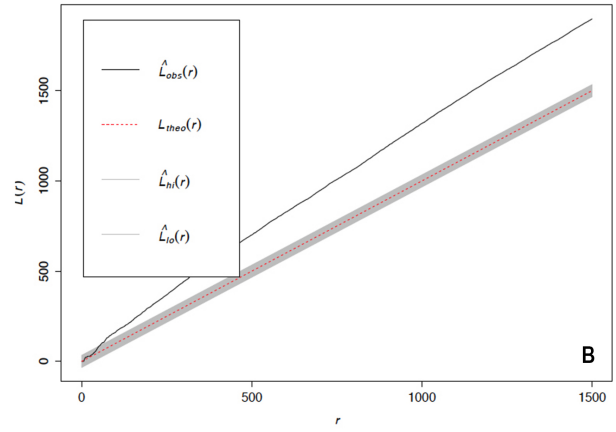
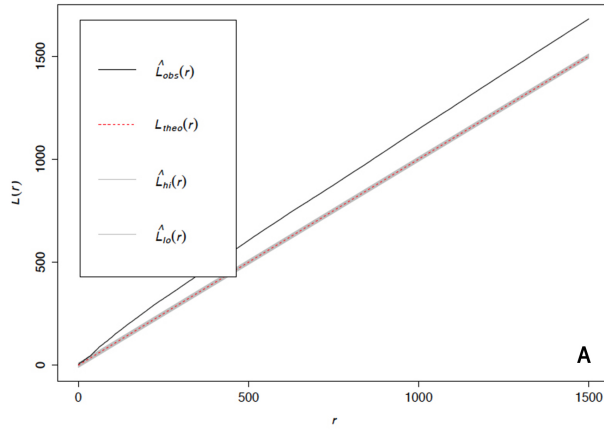


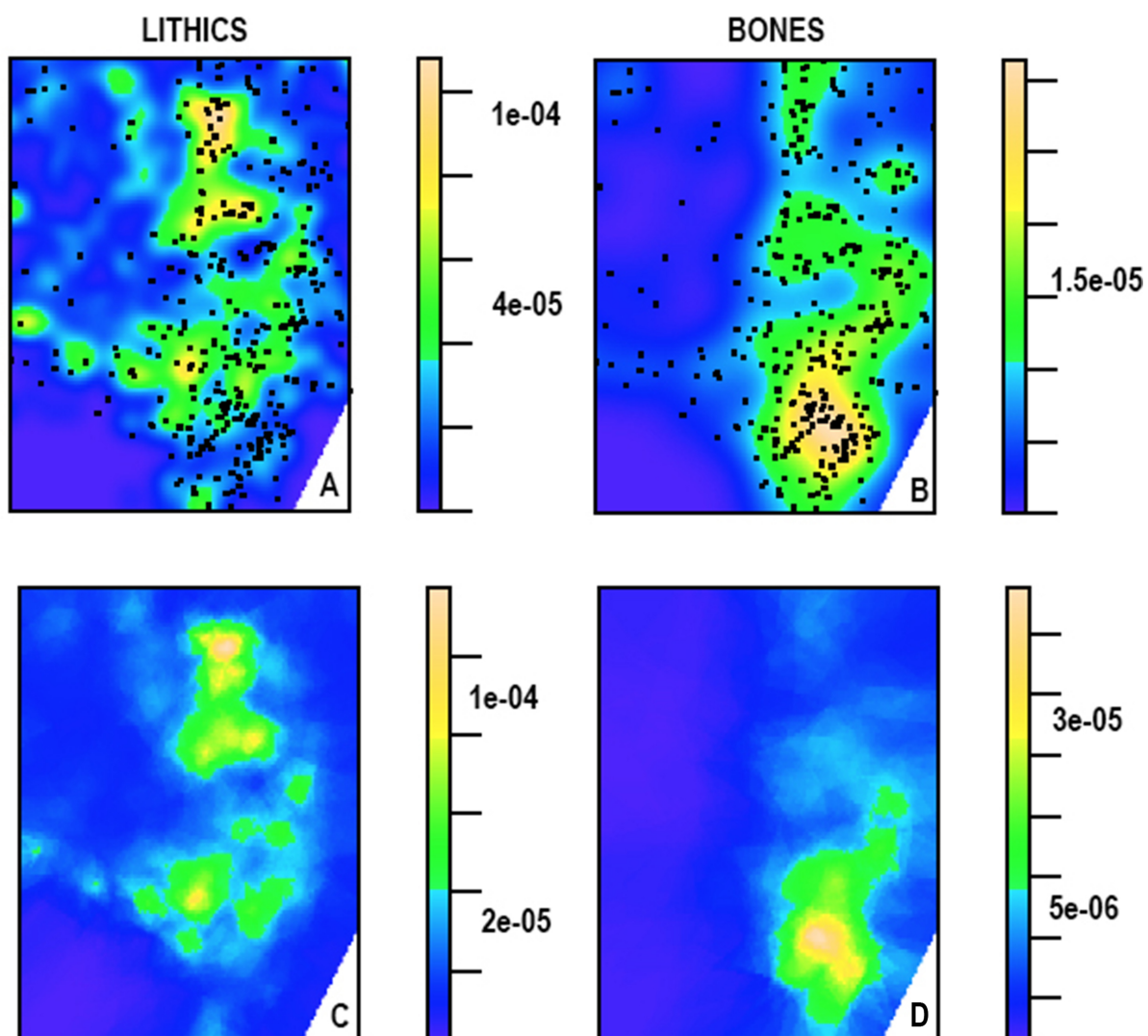


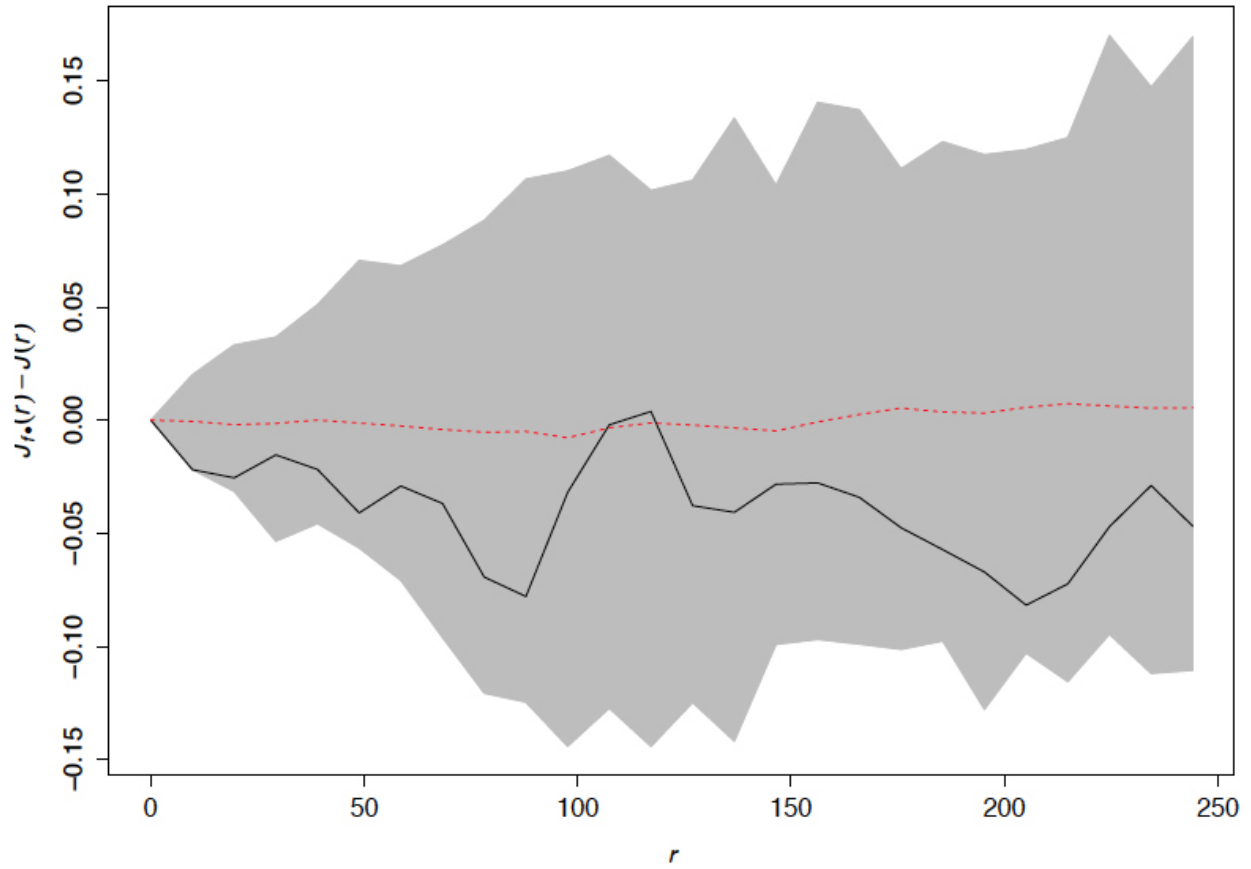




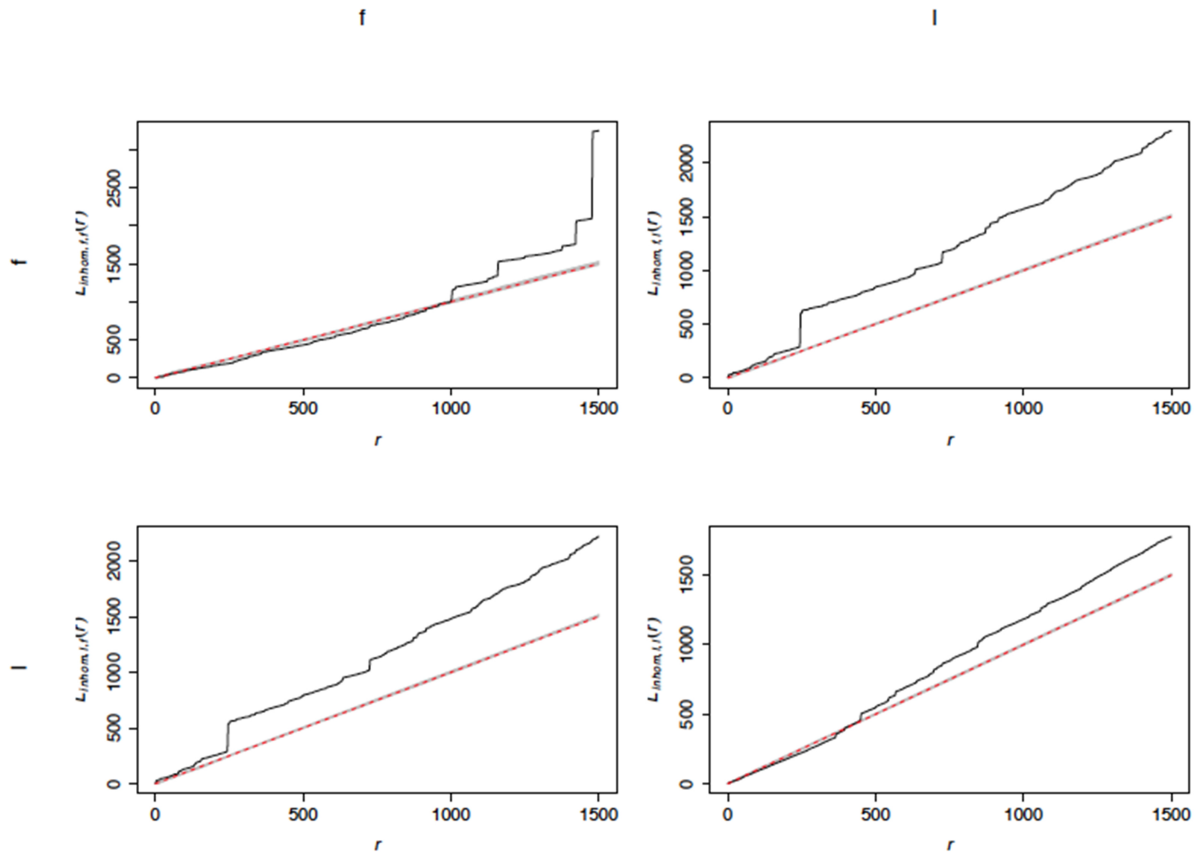
proof







Journal



Journal

Quaternary International

We the authors declare that the manuscript entitled “Assessing functionality during the early Acheulean in level TKSf at Thiongo Korongo site (Olduvai Gorge, Tanzania)” has not any conflict of interest.

Sincerely,

A handwritten signature in blue ink, appearing to read 'J. Panera', with a long horizontal stroke extending to the right.

Joaquín Panera
On behalf of all authors

Journal Pre-proof